Electronic Supplementary Material (ESI) for ChemComm.

Electronic Supplementary Information

Construction of photofunctional peptide conjugates through selective modification of N-terminal cysteine with cyclometallated iridium(III) 2-formylphenylboronic acid complexes for organelle-specific imaging, enzyme activity sensing and photodynamic therapy

Lili Huang,[a] Lawrence Cho-Cheung Lee,[ab] Justin Shum,[a] Guang-Xi Xu[a] and Kenneth Kam-Wing Lo[abc]

[a] Department of Chemistry, City University of Hong Kong, Tat Chee Avenue, Kowloon, Hong Kong, P. R. China; E-mail: bhkenlo@cityu.edu.hk.

[b] Laboratory for Synthetic Chemistry and Chemical Biology Limited, Units 1503-1511, 15/F, Building 17 W, Hong Kong Science Park, New Territories, Hong Kong, P. R. China.

[c] State Key Laboratory of Terahertz and Millimetre Waves, City University of Hong Kong, Tat Chee Avenue, Kowloon, Hong Kong, P. R. China.

Table of Contents

Experimental Section

Materials and Synthesis

All solvents were of analytical reagent grade and purified according to standard procedures.[1] Sodium borohydride, hydrogen bromide, 2-bromo-5-hydroxybenzaldehyde, sodium carbonate, bis(pinacolato) diboron, potassium acetate, potassium carbonate, Pd(dppf)Cl_2, sodium carbonate, sodium periodate, phenol, anhydrous sodium sulfate, tris(2-carboxyethyl)phosphine (TCEP), trifluoroacetic acid (TFA), 1,3-diphenylisobenzofuran (DPBF), L-cysteine (L-Cys), L-lysine (L-Lys), L-methionine (L-Met) and L-serine (L-Ser) were sourced from Acros. Selenium dioxide, 4,4'-dimethyl-2,2'-bipyridine, sodium metabisulfite, $IrCl_3 \cdot H_2O$, 2-phenylphyridine (Hppy), 2-phenylquinonline (Hpq) and 3-(4,5-dimethylthiazol-2-yl)-2,5-diphenyltetrazolium bromide (MTT) were purchased from Sigma-Aldrich. The peptides CKDEL (ER), CSDYQRL (GA) and CGGGGRVRRSVK (FC) were obtained from GL Biochem. The chemicals were directly used with no further purification. The ligands 2-phenylquinonline (Hpqe),[2] 4-bromomethyl-4'-methyl-2,2'-bipyridine (bpy-CH_2-Br),[3] 4-phenoxymethyl-4'-methyl-2,2'-bipyridine (bpy-Ph),[4] 2-(4,4,5,5-tetramethyl-1,3,2-dioxaborolan-2-yl)-5-hydroxybenzaldehyde (Ph-aldh-bae-OH)[5] and the iridium(III) dimer $[Ir_2(N\hat{}C)_4Cl_2]$ (HN^C = Hppy, Hpq and Hpqe)[6] were synthesised according to previous procedures. The buffer components were used as received and were of biological grade. Autoclaved Milli-Q H_2O was used for the preparation of the aqueous solutions. HeLa and HEK 293 cells were obtained from American Type Culture Collection. QSY7 carboxylic acid succinimidyl ester (QSY7-NHS), Dulbecco's Modified Eagle Medium (DMEM), fetal bovine serum (FBS), penicillin/streptomycin, phosphate-buffered saline (PBS), Hank's Balanced Salt Solution (HBSS), trypsin-EDTA, human furin

recombinant, MitoTracker Deep Red, ER-Tracker Green, BODIPY FL C_5-ceramide complexed to BSA, LysoTracker Deep Red, LysoTracker Green, CellMask Deep Red, CM-H_2DCFDA, Rhodamine 123, CellEvent Caspase-3/7 Red, Alexa Fluor 647-Annexin V conjugate, annexin V binding buffer and propidium iodide (PI) were purchased from Invitrogen. Hoechst 33342 was sourced from Abcam.

2-(4,4,5,5-Tetramethyl-1,3,2-dioxaborolan-2-yl)-5-hydroxybenzaldehyde (bpy-Ph-aldh-bae)

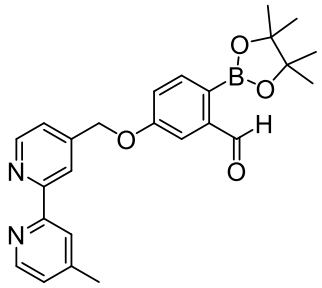

A mixture of Ph-aldh-bae-OH (248 mg, 1 mmol), bpy-CH_2-Br (263 mg, 1 mmol) and K_2CO_3 (209 mg, 1.5 mmol) in DMF (1 mL) was stirred at 298 K for 18 h and then quenched with H_2O (15 mL). The resulting mixture was extracted with EtOAc (15 $\times$ 3 mL). The combined organic extract was washed with brine solution (10 mL), dried over anhydrous sodium sulfate and filtered. The solvent was removed under reduced pressure and the residual yellow solid was purified by column chromatography on silica gel using CH_2Cl_2/MeOH (100:1, *v*/*v*) as the eluent. The solvent was removed under reduced pressure to afford the product as a white solid. Yield: 224 mg (52%). ^{1}H NMR (400 MHz, $CDCl_3$, 298 K, TMS): δ 10.68 (s, 1H, CHO), 8.72 (d, *J* = 4.8 Hz, 1H, H6 of bpy), 8.61 – 8.59 (m, 2H, H6’ and H3 of bpy), 8.33 (s, 1H, H3’ of bpy), 7.91 (d, *J* = 8.2 Hz, 1H, H5 of phenyl ring of bpy-Ph-aldh-bae), 7.60 (s, 1H, H2 of phenyl ring of bpy-Ph-aldh-bae), 7.45 (d, *J* = 4.8 Hz, 1H, H5 of bpy), 7.28 – 7.24 (m, 2H, H5’ of bpy and H6 of phenyl ring of bpy-Ph-aldh-bae), 5.28 (s, 2H, CH_2 of bpy-Ph-aldh-bae), 2.51 (s, 3H, CH_3 of bpy), 1.39 (s, CH_3 of pinacol ester of bpy-Ph-aldh-bae). ESI-MS (positive-ion mode): *m*/*z* 431 $[M + H^+]^+$.

4-((3-Formyl-4-boronophenyl)oxymethyl)-4'-methyl-2,2'-bipyridine (bpy-2-FPBA)

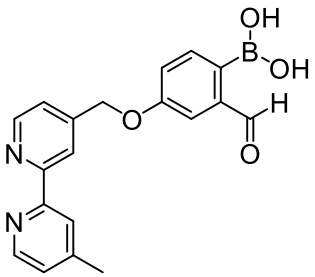

To a mixture of bpy-2-FPBA (430 mg, 1 mmol) in THF (1 mL) and H_2O (0.4 mL), $NaIO_4$ (636 mg, 1.5 mmol) was added and the resulting solution was stirred at 298 K for 15 min. After addition of HCl (1 N, 1 mL), the mixture was further stirred for 4 h and then extracted with EtOAc (30 mL $\times$ 3). The combined organic extract was washed with brine solution (30 mL), dried over anhydrous sodium sulfate and filtered. The solutions were reduced in vacuum to 1 mL and then hexane (20 mL) was added to precipitate the product. A white solid was obtained by filtration and used without further purification. Yield: 69.8 mg (20%). ^{1}H NMR (400 MHz, DMSO-d_6, 298 K, TMS): δ10.20 (s, 1H, CHO), 8.70 (d, J = 4.9 Hz, 1H, H6 of bpy), 8.57 (d, J = 4.9 Hz, 1H, H6' of bpy), 8.48 (s, 1H, H3 of bpy), 8.28 (s, 1H, H3' of bpy), 7.64 (d, J = 8.2 Hz, 1H, H5 of phenyl bpy-2-FPBA), 7.54 – 7.51 (m, 2H, H5 of bpy and H2 of phenyl bpy-2-FPBA), 7.35 – 7.33 (m, 2H, H5' of bpy and H6 of phenyl bpy-2-FPBA), 5.41 (s, 2H, CH_2 of bpy-2-FPBA), 2.44 (s, 3H, CH_3 of bpy). ESI-MS (positive-ion mode): m/z 349 $[M + H^+]^+$.

$[Ir(ppy)_2(bpy\text{-}2\text{-}FPBA)](PF_6)$ (**1a**)

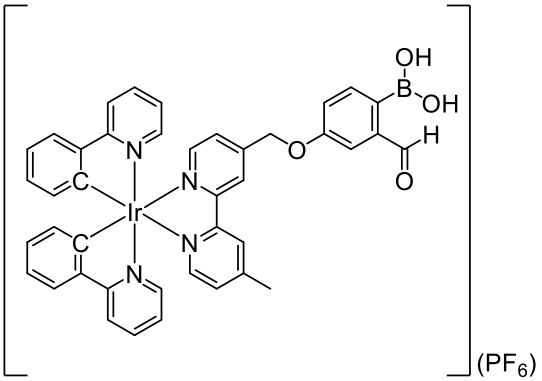

A mixture of $[Ir_2(ppy)_4Cl_2]$ (76.4 mg, 0.06 mmol) and bpy-2-FPBA (41.8 mg, 0.12 mmol) in CH_2Cl_2/MeOH (20 mL) (1:1, *v*/*v*) was stirred at 298 K under an inert atmosphere of nitrogen in the dark for 18 h. After the addition of solid KPF_6 (17.4 mg, 0.12 mmol), the mixture was further stirred for 2 h. The solvent was removed under reduced pressure and the residual yellow solid was purified by column chromatography on silica gel using CH_2Cl_2/MeOH (100:1, *v*/*v*) as the eluent. The solvent was removed under reduced pressure to give a yellow solid. Subsequent recrystallisation of the solid from CH_2Cl_2/Et_2O afforded the complex as yellow crystals. Yield: 45.9 mg (65%). ^{1}H NMR (300 MHz, DMSO-d_6, 298 K, TMS): δ 10.27 (s, 1H, CHO), 8.96 (s, 1H, H3 of bpy), 8.82 (s, 1H, H3’ of bpy), 8.29 – 8.26 (m, 2H, H3 and H3’ of pyridyl ring of ppy), 7.97 – 7.86 (m, 5H, H6 and H6’ of bpy, H3 and H3’ of phenyl ring of ppy, and H5 of bpy), 7.77 (d, *J* = 5.6 Hz, 1H, H5 of phenyl ring of bpy-2-FPBA), 7.72 – 7.64 (m, 4H, H6 and H6’ of pyridyl ring of ppy and H4 and H4’ of pyridyl ring of ppy), 7.56 – 7.52 (m, 2H, H2 of phenyl ring of bpy-2-FPBA and H5’ of bpy), 7.39 – 7.35 (m, 1H, H6 of phenyl ring of bpy-2-FPBA), 7.19 – 7.15 (m, 2H, H5 and H5’ of pyridyl ring of ppy), 7.05 – 7.00 (m, 2H, H4 and H4’of phenyl ring of ppy), 6.90 (t, *J* = 7.4 Hz, 2H, H5 and H5’ of phenyl ring of ppy), 6.22 – 6.18 (m, 2H, H6 and H6’ of phenyl ring of ppy), 5.44 (s, 2H, CH_2 of bpy-2-

FPBA), 2.55 (s, 3H, CH_3 of bpy). ^{13}C NMR (150 MHz, DMSO-d_6, 298 K, TMS): δ 194.6, 167.3, 158.9, 156.1, 155.2, 152.1, 151.1, 150.3, 149.6, 149.3, 144.3, 142.0, 139.2, 136.4, 131.6, 131.5, 130.7, 129.9, 126.9, 126.3, 125.6, 124.4, 123.1, 122.7, 120.5, 120.4, 113.4, 67.9, 21.4. IR (KBr) $\tilde{\nu}$/cm^{-1}: 3446 (O–H), 1706 (C=O), 845 (PF_6^-). HR-ESI-MS (positive-ion mode, *m*/*z*): $[M - PF_6^-]^+$ calcd for $IrC_{41}H_{33}BN_4O_4$ 849.2224, found 849.2180.

$[Ir(ppy)_2(bpy\text{-}Ph)](PF_6)$ (**1b**)

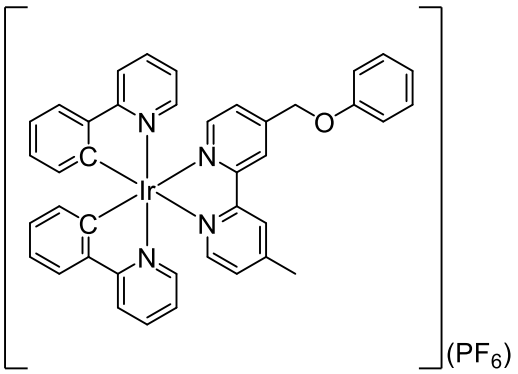

A mixture of $[Ir_2(ppy)_4Cl_2]$ (76.4 mg, 0.06 mmol) and bpy-Ph (33.2 mg, 0.12 mmol) in CH_2Cl_2/MeOH (20 mL) (1:1, *v*/*v*) was stirred under an inert atmosphere of nitrogen in the dark for 18 h. After the addition of solid KPF_6 (17.4 mg, 0.12 mmol), the mixture was further stirred for 2 h. The solvent was removed under reduced pressure and the residual yellow solid was purified by column chromatography on silica gel using CH_2Cl_2/MeOH (100:1, *v*/*v*) as the eluent. The solvent was removed under reduced pressure to give a yellow solid. Subsequent recrystallisation of the solid from CH_2Cl_2/Et_2O afforded the complex as yellow crystals. Yield: 41.5 mg (75%). ^1H NMR (300 MHz, DMSO-d_6, 298 K, TMS): δ 8.94 (s, 1H, H3 of bpy), 8.82 (s, 1H, H3’ of bpy), 8.29 – 8.26 (m, 2H, H3 and H3’ of pyridyl ring of ppy), 7.97 – 7.91 (m, 4H, H6 and H6’ of bpy and H3 and H3’ of phenyl ring of ppy), 7.87 (d, *J* = 5.7 Hz, 1H, H6 of pyridyl ring

of ppy), 7.76 (d, *J* = 5.6 Hz, 1H, H5 of bpy), 7.70 (d, *J* = 5.7 Hz, 1H, H6' of pyridyl ring of ppy), 7.67 – 7.63 (m, 2H, H3 and H5 of phenyl ring of bpy-Ph), 7.55 (d, *J* = 5.6 Hz, 1H, H5' of bpy), 7.38 – 7.33 (m, 2H, H2 and H6 of phenyl ring of bpy-Ph), 7.19 – 7.15 (m, 2H, H4 and H4'of pyridyl ring of ppy), 7.10 – 7.00 (m, 5H, H4 and H4'of phenyl ring of ppy, H5 and H5' of phenyl ring of ppy and H4 of phenyl ring of bpy-Ph), 6.90 (t, *J* = 7.4 Hz, 2H, H5 and H5' of phenyl ring of ppy), 6.22 – 6.18 (m, 2H, H6 and H6' of phenyl ring of ppy), 5.33 (s, 2H, CH_2 of bpy-Ph), 2.55 (s, 3H, CH_3 of bpy). ^{13}C NMR (150 MHz, DMSO-d_6, 298 K, TMS): δ167.3, 167.2, 158.2, 156.1, 155.3, 152.1, 151.1, 151.0, 150.7, 150.3, 149.6, 149.3, 149.3, 144.2, 144.2, 139.2, 130.2, 127.0, 126.3, 125.6, 125.5, 124.4, 123.3, 122.7, 121.9, 120.5, 115.3, 67.8, 21.4. IR (KBr) $\tilde{\nu}$/cm^{-1}: 844 (PF_6^-). HR-ESI-MS (positive-ion mode, *m*/*z*): $[M - PF_6^-]^+$ calcd for $IrC_{40}H_{32}N_4O$ 777.2205, found 777.2222.

$[Ir(pq)_2(bpy\text{-}2\text{-}FPBA)](PF_6)$ (**2a**)

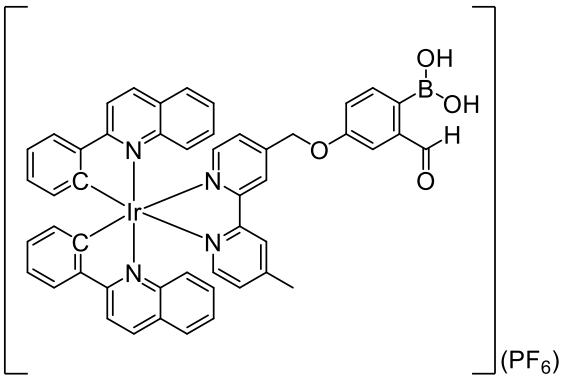

The synthetic procedure was similar to that of complex **1a**, except that $[Ir_2(pq)_4Cl_2]$ (38.1 mg. 0.03 mmol) was used instead of $[Ir_2(ppy)_4Cl_2]$. Subsequent recrystallisation of the solid from CH_2Cl_2/Et_2O afforded the complex as orange crystals. Yield: 45.9 mg (70%). ^{1}H NMR (300 MHz, DMSO-d_6, 298 K, TMS): δ10.24 (s, 1H, CHO), 8.59 – 8.52 (m, 5H, H3 of bpy, H4 and H4' of quinolinyl ring of pq, and H3 and H3' of quinolinyl ring of

pq), 8.40 (s, 1H, H3’ of bpy), 8.29 (d, *J* = 8.0 Hz, 2H, H3 and H3’ of phenyl ring of pq), 8.10 (d, *J* = 5.8 Hz, 1H, H6 of bpy), 7.95 – 7.93 (m, 3H, H6’ of bpy and H8 and H8’ of quinolinyl ring of pq), 7.74 (d, *J* = 5.6 Hz, 1H, H5 of bpy), 7.66 – 7.64 (m, 1H, H5 of phenyl ring of bpy-2-FPBA), 7.54 (d, *J* = 5.6 Hz, 1H, H5’ bpy), 7.45 – 7.38 (m, 3H, H2 of phenyl ring of bpy-2-FPBA and H5 and H5’ of quinolinyl ring of pq), 7.26 – 7.23 (m, 2H, H7 and H7’ of quinolinyl ring of pq), 7.18 – 7.11 (m, 4H, H6 and H6’ of quinolinyl ring of pq and H4 and H4’ of phenyl ring of pq), 6.98 – 6.95 (m, 1H, H6 of phenyl ring of bpy-2-FPBA), 6.82 (t, *J* = 7.5 Hz, 2H, H5 and H5’ of phenyl ring of pq), 6.40 (m, 2H, H6 and H6’ of phenyl ring of pq), 5.36 (s, 2H, CH_2 of bpy-2-FPBA), 2.43 (s, 3H, CH_3 of bpy). ^{13}C NMR (150 MHz, DMSO-d_6, 298 K, TMS): δ 194.5, 170.2, 158.6, 155.7, 154.8, 152.3, 151.6, 150.7, 147.8, 147.3, 147.2, 147.1, 146.3, 142.0, 140.9, 136.3, 134.2, 131.5, 131.3, 131.0, 129.9, 129.7, 128.2, 128.1, 127.9, 127.2, 126.5, 125.5, 124.6, 124.4, 123.1, 122.3, 120.4, 118.7, 113.4, 67.4, 21.2. IR (KBr) $\tilde{\nu}$/cm^{-1}: 3445 (O–H), 1706 (C=O), 845 (PF_6^-). HR-ESI-MS (positive-ion mode, *m*/*z*): $[M - PF_6^-]^+$ calcd for $IrC_{49}H_{37}BN_4O_4$ 949.2537, found 949.2555.

$[Ir(pq)_2(bpy\text{-}Ph)](PF_6)$ (**2b**)

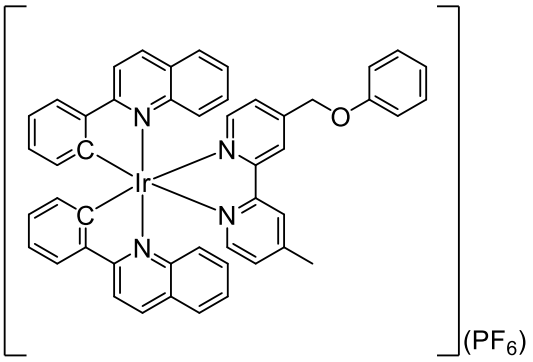

The synthetic procedure was similar to that of complex **1b**, except that $[Ir_2(pq)_4Cl_2]$ (38.1 mg. 0.03 mmol) was used instead of $[Ir_2(ppy)_4Cl_2]$. Subsequent recrystallisation

of the solid from CH_2Cl_2/Et_2O afforded the complex as orange crystals. Yield: 46.6 mg (76%). ^{1}H NMR (400 MHz, acetone-d_6, 298 K, TMS): δ 8.55 – 8.54 (m, 5H, H3 of bpy-Ph, H4 and H4’ of quinolinyl ring of pq, H3 and H3’ of quinolinyl ring of pq), 8.37 (s, 1H, H3’ of bpy-Ph), 8.34 (d, *J* = 5.7 Hz, 1H, H6 of bpy-Ph), 8.26 (d, *J* = 7.9 Hz, 2H, H3 and H3’ of phenyl ring of pq), 8.20 (d, *J* = 5.7 Hz, 1H, H6’ of bpy-Ph), 7.97 – 7.94 (m, 2H, H8 and H8’ of quinolinyl ring of pq), 7.80 (d, *J* = 5.0 Hz, 1H, H5 of bpy), 7.57 (d, *J* = 5.0 Hz, 1H, H5’ of bpy), 7.49 – 7.40 (m, 4H, H2, H3, H5 and H6 of phenyl ring of bpy-Ph), 7.34 – 7.30 (m, 2H, H5 and H5’ of quinolinyl ring of pq), 7.20 – 7.13 (m, 3H, H4 of phenyl ring of bpy-Ph, and H7 and H7’ of quinolinyl ring of pq), 7.06 – 6.96 (m, 4H, H4 and H4’ of phenyl ring of pq and H6 and H6’ of quinolinyl ring of pq), 6.86 (t, *J* = 7.5 Hz, 2H, H5 and H5’ of phenyl ring of pq), 6.59 – 6.57 (m, 2H, H6 and H6’ of phenyl ring of pq), 5.32 (s, 2H, CH_2 of bpy-Ph), 2.49 (s, 3H, CH_3 of bpy). ^{13}C NMR (150 MHz, DMSO-d_6, 298 K, TMS): δ 170.2, 157.8, 155.6, 154.8, 152.2, 151.6, 151.1, 147.8, 147.3, 147.2, 147.1, 146.3, 140.9, 134.2, 131.5, 131.3, 131.1, 130.1, 129.9, 129.6, 128.2, 128.1, 127.9, 127.2, 126.6, 125.5, 124.6, 124.4, 123.1, 122.5, 121.9, 118.7, 115.4, 67.3, 21.2. IR (KBr) $\tilde{\nu}$/cm^{-1}: 844 (PF_6^-). HR-ESI-MS (positive-ion mode, *m*/*z*): $[M - PF_6^-]^+$ calcd for $IrC_{48}H_{36}N_4O$ 877.2518, found 877.2524.

$[Ir(pqe)_2(bpy\text{-}2\text{-}FPBA)](PF_6)$ (**3a**)

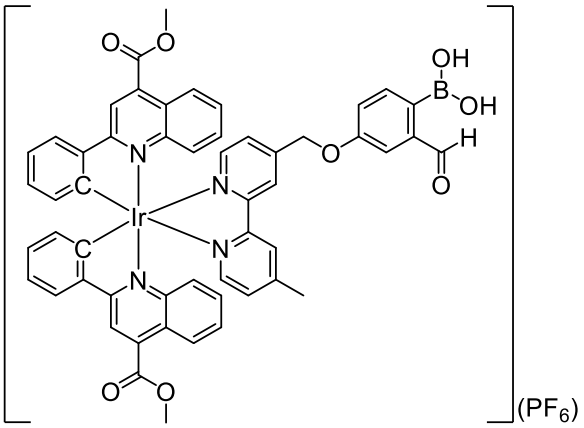

The synthetic procedure was similar to that of complex **1a**, except that $[Ir_2(pqe)_4Cl_2]$ (45.1 mg. 0.03 mmol) was used instead of $[Ir_2(ppy)_4Cl_2]$. Subsequent recrystallisation of the solid from CH_2Cl_2/Et_2O afforded the complex as red crystals. Yield: 50.8 mg (70%). ^{1}H NMR (400 MHz, DMSO-d_6, 298 K, TMS): δ 10.23 (s, 1H, CHO), 8.84 – 8.83 (m, 2H, H3 and H3' of quinolinyl ring of pqe), 8.54 (s, 1H, H3 of bpy), 8.41 – 8.32 (m, 5H, H3'of bpy, and H3 and H3' of phenyl ring of pqe, and H8' and H8' of quinolinyl ring of pqe), 8.09 (d, *J* = 5.7 Hz, 1H, H6 of bpy), 7.93 (d, *J* = 5.7 Hz, 1H, H6' of bpy), 7.76 (d, *J* = 5.8 Hz, 1H, H5 of bpy-2-FPBA), 7.64 (d, *J* = 8.2 Hz, 1H, H5 of bpy-2-FPBA), 7.57 – 7.47 (m, 3H, H5' of bpy and H5 and H5' of quinolinyl ring of pqe), 7.41 – 7.39 (m, 2H, H7 and H7' of quinolinyl ring of pqe), 7.31 – 7.15 (m, 5H, H2 of phenyl ring bpy-2-FPBA, H6 and H6' of quinolinyl ring of pqe, and H4 and H4' of phenyl ring of pqe), 7.03 – 6.99 (m, 1H, H6 of phenyl ring of bpy-2-FPBA), 6.89 – 6.84 (m, 2H, H5 and H5' of phenyl ring of pqe), 6.46 (d, *J* = 7.6 Hz, 2H, H6 and H6' of phenyl ring of pqe), 5.37 (s, 2H, CH_2 of bpy-2-FPBA), 4.07 (s, 6H, CH_3 of pqe), 2.48 (s, 3H, CH_3 of bpy). ^{13}C NMR (150 MHz, DMSO-d_6, 298 K, TMS): δ 194.5, 170.2, 165.8, 158.6, 155.4, 154.6, 152.6, 151.7, 151.1, 147.9, 147.7, 147.1, 145.7, 142.0, 139.6, 136.3, 134.5, 131.7, 130.0, 128.8, 128.6, 126.9, 126.7, 125.6, 125.2, 125.1, 124.0, 123.5, 122.3, 120.4, 119.1,

119.0, 113.3, 67.4, 53.9, 21.2. IR (KBr) $\tilde{\nu}$/cm^{-1}: 3446 (O–H), 1732 (C=O), 843 (PF_6^-). HR-ESI-MS (positive-ion mode, *m*/*z*): $[M - PF_6^-]^+$ calcd for $IrC_{53}H_{41}BN_4O_8$ 1065.2647, found 1065.2643.

$[Ir(pqe)_2(bpy\text{-}Ph)](PF_6)$ (**3b**)

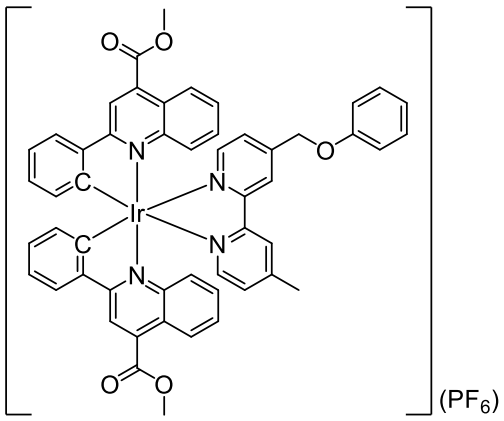

The synthetic procedure was similar to that of complex **1b**, except that $[Ir_2(pqe)_4Cl_2]$ (45.1 mg. 0.03 mmol) was used instead of $[Ir_2(ppy)_4Cl_2]$. Subsequent recrystallisation of the solid from CH_2Cl_2/Et_2O afforded the complex as red crystals. Yield: 49.8 mg (73%). ^{1}H NMR (400 MHz, acetone-d_6, 298 K, TMS): δ8.88 – 8.87 (m, 2H, H3 and H3'of quinolinyl ring of pqe), 8.56 – 8.52 (m, 3H, H3 of bpy and H3 and H3' of phenyl ring of pqe), 8.37 – 8.32 (m, 4H, H8 and H8' of quinolinyl ring of pqe and H3' and H6 of bpy), 8.20 (d, *J* = 5.7 Hz, 1H, H6' of bpy), 7.81 (d, *J* = 5.6 Hz, 1H, H5 of bpy), 7.64 – 7.52 (m, 5H, H5' of bpy and H5, H5', H7 and H7' of quinolinyl ring of pqe), 7.33 – 7.19 (m, 5H, H2, H3 and H6 of phenyl ring of bpy-Ph and H6 and H6' of quinolinyl ring of pqe), 7.12 – 7.08 (m, 1H, H5 of phenyl ring of bpy-Ph), 7.03 – 6.95 (m, 3H, H4 of phenyl ring of bpy-Ph and H4 and H4' of phenyl ring of pqe), 6.97 (d, *J* = 8.0 Hz, 2H, H2 and H6 of phenyl ring of bpy-Ph), 6.89 – 6.87 (m, 2H, H5 and H5' of phenyl ring of pqe), 6.65 (d, *J* = 7.6 Hz, 2H, H6 and H6' of phenyl ring of pqe), 5.32 (s, 2H, CH_2 of bpy-Ph), 4.14 (s, 6H, CH_3 of pqe), 2.48 (s, 3H, CH_3 of bpy). ^{13}C NMR (150 MHz, DMSO-d_6, 298 K, TMS):

δ 170.2, 170.1, 165.8, 157.8, 155.4, 154.6, 152.6, 151.7, 151.4, 147.8, 147.7, 147.1, 145.6, 139.6, 139.5, 134.5, 131.8, 131.7, 131.6, 130.1, 129.9, 128.8, 128.7, 128.6, 126.9, 126.8, 125.6, 125.2, 125.1, 124.0, 123.5, 122.5, 121.9, 119.1, 119.0, 115.4, 67.3, 65.4, 53.9, 53.8, 21.2, 15.6. IR (KBr) $\tilde{\nu}$/cm^{-1}: 845 (PF_6^-). HR-ESI-MS (positive-ion mode, *m*/*z*): $[M - PF_6^-]^+$ calcd for $IrC_{52}H_{40}N_4O_5$ 993.2628, found 993.2654.

Preparation of the Cysteine and Peptide Conjugates of Complex 1a

A mixture of complex **1a** (2 μmol) and L-Cys or the cysteine-containing peptides (3 μmol) in acetate ammonium buffer (50 mM, pH 7.4)/DMF (1:1, *v*/*v*, 1 mL) containing TCEP (12 μmol) was stirred at 37°C in the dark for 12 h. The solvent was removed under reduced pressure and the residual solid was purified by semi-preparative RP-HPLC. The purified product was analysed by an Agilent analytical column (ZORBAX Eclipse Plus C18: 4.6 × 150 mm, 5 μm) with a linear gradient of 30 – 100% B over 18 min and a flow rate of 1 mL min^{-1}. **1a-Cys**. Yield: 1.7 mg (82%). Positive-ion ESI-MS ion clusters at *m*/*z* 934.9 $[M - CF_3CO_2^-]^+$. **1a-ER**. Yield: 2.5 mg (81%). Positive-ion ESI-MS ion clusters at *m*/*z* 761.5 $[M - CF_3CO_2^- + H^+]^{2+}$. **1a-GA**. Yield: 3.0 mg (82%). Positive-ion ESI-MS ion clusters at *m*/*z* 899.3 $[M - CF_3CO_2^- + H^+]^{2+}$. **1a-FC**. Yield: 3.6 mg (83%). Positive-ion ESI-MS ion clusters at *m*/*z* 682.5 $[M - CF_3CO_2^- + 2H^+]^{3+}$, 512.1 $[M - CF_3CO_2^- + 3H^+]^{4+}$. For the QSY7-containing conjugate, a mixture of the purified **1a-FC** (1 μmol), QSY7-NHS (2 μmol) and Et_3N (5 μmol) in DMF (500 μL) was stirred at 37°C under an inert atmosphere of nitrogen in the dark for 18 h. The solvent was removed under reduced pressure and the residual solid was further purified by semi-preparative RP-HPLC. **1a-FC-QSY7**. Yield: 2.4 mg (85%). ESI-MS ion clusters at *m*/*z* 895.6 $[M - CF_3CO_2^- + 2H^+]^{3+}$, 672.2 $[M - CF_3CO_2^- + 3H^+]^{4+}$, 538.1 $[M - CF_3CO_2^- + 4H^+]^{5+}$.

Physical Measurements and Instrumentation

^{1}H and ^{13}C NMR spectra were recorded on a Bruker AVANCE III 300, 400, or 600 MHz spectrometer at 298 K using deuterated solvents. Chemical shifts (δ, ppm) were reported relative to tetramethylsilane (TMS). Positive-ion electrospray ionisation mass spectra (ESI-MS) were recorded on a Perkin-Elmer Sciex API 3200MD mass spectrometer. High-resolution electrospray ionisation mass spectra (HR-ESI-MS) were recorded on a Bruker micrOTOF-QII. IR spectra of the samples in KBr pellets were recorded in the range of 4000 – 400 cm^{-1} using a Perkin Elmer FTIR–1600 spectrometer. Electronic absorption spectra were recorded on an Agilent 8453 diode array spectrophotometer. Steady-state emission spectra were recorded on a HORIBA FluoroMax-4 spectrofluorometer. Unless specified otherwise, all solutions for photophysical studies were degassed with no fewer than four successive freeze-pump-thaw cycles and stored in a 10-cm^3 round bottomed flask equipped with a side-arm 1-cm fluorescence cuvette and sealed from the atmosphere by a Rotaflo HP6/6 quick-release Teflon stopper. Emission quantum yields (Φ_{em}) were measured by optically dilute method using an aerated aqueous solution of the $[Ru(bpy)_3]Cl_2$ (Φ_{em} = 0.040, λ_{ex} = 455 nm) as the standard solution.[7] The concentrations of the standard and sample solutions were adjusted until the absorbance at 455 nm was 0.1. Emission lifetimes were measured on an Edinburgh Instruments LP920 laser flash photolysis spectrometer using the third harmonic output (355 nm; 6 – 8 ns fwhm pulse width) of a Spectra-Physics Quanta-Ray Q-switched LAB-150 pulsed Nd:YAG laser (10 Hz) as the excitation source. High performance liquid chromatography (HPLC) was performed on an Agilent 1260 Infinity II system coupled with a diode array detector WR. HPLC was performed on an Agilent 1260 Infinity II system coupled with a diode array detector

WR using H_2O containing 0.1% (*v*/*v*) trifluoroacetic acid (TFA) (solvent A) and CH_3CN containing 0.1% (*v*/*v*) TFA (solvent B) as the solvents. The HPLC analyses were carried out using an Agilent analytical column (ZORBAX Eclipse Plus C18: 4.6 × 150 mm, 5 μm) with a linear gradient of 10 to 100% B and a flow rate of 1 mL min^{-1} and the detector was set at 210 or 350 nm. The HPLC purifications were performed on an Agilent semi-preparative column (ZORBAX Eclipse XDB-C18 column: 9.4 × 250 mm, 5 μm) with a linear gradient of 50 – 100% B over 20 min and a flow rate of 3 mL min^{-1}.

Kinetics Studies

All reactions were performed on a 100-μL scale. The reaction kinetics of the ligand bpy-FPBA and FPBA complexes **1** – **3** (25 μM) with L-Cys (125 μM) in ammonium acetate buffer (50 mM, pH 7.4)/DMF (9:1, *v*/*v*) containing TCEP (500 μM) at 298 K was measured by RP-HPLC. The reactions at different time points were quenched by the addition of 900 μL of H_2O/ CH_3CN (1:1, *v*/*v*) containing 0.1% TFA and then analysed by RP-HPLC. The second-order rate constants (k_2) were determined by fitting the data to the following equation:

$$y = \frac{ln\frac{[A]_o[B]_t}{[A]_t[B]_o}}{([B]_o - [A]_o)} = k_2 t$$

where $[A]_o$ and $[A]_t$ are the concentrations of the FPBA-containing compound (ligand or complex) at time = 0 and *t* s, respectively; and $[B]_o$ and $[B]_t$ are the concentrations

of cysteine at time = 0 and *t* s, respectively. All kinetic curves generated using OriginPro 8.0 software package are summarised in Fig. S5.

Determination of $^1O_2$ Generation Quantum Yields (Φ_Δ)

The $^1O_2$ generation quantum yields were determined by detecting the oxidation of DPBF using absorbance measurements.[8] An aerated MeOH solution (2 mL) containing the iridium(III) complexes and DPBF (100 μM) was introduced to a 1-cm path length quartz cuvette and irradiated at 450 nm using a Xenon lamp (Ushio) (150 W) with a bandwidth of 20 nm. $[Ru(bpy)_3]Cl_2$ was used as a reference for $^1O_2$ sensitisation (Φ_Δ = 0.73 in MeOH).[9] The absorbance of DPBF at *ca.* 418 nm would decrease upon the irreversible 1,4-cycloaddition reaction of DPBF induced by $^1O_2$.

The following equation was used for the calculation of Φ_Δ:

$$\Phi_\Delta^{unknown} = \Phi_\Delta^{reference} \times \frac{m^{unknown} \times F^{reference}}{m^{reference} \times F^{unknown}}$$

where *m* is the slope of a linear fit of the change of absorbance at 418 nm against the irradiation time and *F* is the absorption correction factor, which is given as $F = 1 - 10^{-AL}$ (*A* = absorbance at 450 nm and *L* = path length of the cuvette).

Selectivity Studies

For the chemoselectivity studies, complex **1a** (25 nmol) in anhydrous DMF (100 μL) was added to a mixture of L-Cys, L-Lys, L-Met and L-Ser (100 nmol) in ammonium acetate buffer (50 mM, pH 7.4) (900 μL) containing TCEP (400 nM). The mixture was incubated in the dark at 37°C for 4 h. An aliquot of the reaction mixture (20 μL) was analysed by RP-HPLC. For the regioselectivity studies, complex **1a** (25 nmol) in

anhydrous DMF (100 μL) was added to the tripeptide CSS, SCS, or SSC (100 nmol) in ammonium acetate buffer (50 mM, pH 7.4, 900 μL) containing TCEP (400 nmol).

Förster Distance Measurements

The Förster distance (R_o) between the iridium donor (D) and QSY7 acceptor (A) was calculated according to the following equation:

$$R_o(\text{in Å}) = 0.211 \times \sqrt[6]{\kappa^2 \times n^{-4} \times \Phi_D \times J(\lambda)}$$

where k^2 is a factor describing the relative orientation in space of the transition dipoles of the D and the A and is assumed to be 2/3; n is the refractive index of the solvent; Φ_D is the emission quantum yield of **1a-FC**; $J(\lambda)$ is the overlap integral of the donor **1a-FC** emission and the acceptor QSY7 absorption spectra.

Calculation of $J(\lambda)$ is based on the equation below:

$$J(\lambda) = \int_0^\infty F_D(\lambda) \times \varepsilon_A(\lambda) \times \lambda^4 \, d\lambda$$

where F_D is the corrected emission intensity of the donor **1a-FC** with the emission intensity normalised to unity and ε_A is the absorption coefficient of the acceptor.

Calculated energy transfer efficiency (E_{calc}) based on Förster's theory was determined according to the following equation:

$$E_{calc} = \frac{R_o^6}{R_o^6 + r^6}$$

where r is the distance between the iridium(III) metal centre and the QSY7 moiety, which was estimated by the three-dimensional structures of the conjugate **1a-FC-QSY** modulated by Chem3D 16.0.

Experimentally determined energy transfer efficiency (E_{expt}) was determined on the basis of the emission quantum yields of **1a-FC** and **1a-FC-QSY** according to the

following equation:

$$E_{expt} = 1 - (\Phi_{em,1a-FC-QSY7} / \Phi_{em,1a-FC})$$

Cell Cultures

HeLa and HEK 293 cells were cultured in DMEM containing 10% FBS and 1% penicillin/streptomycin in an incubator at 37°C under a 5% CO_2 atmosphere. Cells were passaged by dissociation from the adherent state with 0.25% trypsin in PBS (pH 7.4) to retain their viability when 70 – 80% confluence was reached.

Cellular Uptake

HeLa and HEK 293 cells were grown in a 35-mm tissue culture dish and incubated at 37°C under a 5% CO_2 atmosphere for 48 h. The culture medium was removed and replaced with a fresh medium containing the conjugates of complex **1a** (10 μM, 4 h) at 37°C under a 5% CO_2 atmosphere and the cells were washed with PBS (1 mL × 3). The cells were then trypsinised and harvested with PBS (1 mL). The cell number was counted with a Logos Biosystems LUNA-II automated cell counter. The harvested cells were digested with 65% HNO_3 (1 mL) at 60°C for 2 h, allowed to cool to room temperature and analysed by a NexION 2000 ICP-MS instrument (PerkinElmer SCIEX Instruments).

Live-cell Confocal Imaging

HeLa cells in growth medium were seeded on a sterilised coverslip in a 35-mm tissue culture dish and grown at 37°C under a 5% CO_2 atmosphere for 48 h. In the mitochondria and ER co-staining experiments, after treatment with **1a-Cys** or **1a-ER** (20 μM, 4 h, λ_{ex} = 405 nm, λ_{em} = 550 – 650 nm), the cells were washed with PBS (1 mL

× 3) and further incubated with MitoTracker Deep Red (100 nM, 20 min, λ_{ex} = 635 nm, λ_{em} = 650 – 680 nm), MitoTracker Green (100 nM, 20 min, λ_{ex} = 488 nm, λ_{em} = 500 – 550 nm), ER-Tracker Green (1 μM, 20 min, λ_{ex} = 488 nm, λ_{em} = 500 – 550 nm), LysoTracker Deep Red (100 nM, 30 min, λ_{ex} = 635 nm, λ_{em} = 650 – 680 nm) or LysoTracker Green (100 nM, 30 min, λ_{ex} = 488 nm, λ_{em} = 500 – 550 nm) in growth medium at 37°C under a 5% CO_2 atmosphere. After washing with PBS (1 mL × 3), the cells were imaged using a Leica TCS SPE (inverted configuration) confocal microscope with an oil immersion 63x oil-immersion objective lens. In the GA co-staining experiment, after treatment with **1a-GA** (20 μM, 16 h, λ_{ex} = 405 nm, λ_{em} = 550 – 650 nm), the cells were washed with Hank's Balanced Salt Solution (HBSS) (1 mL × 3) and then incubated with BODIPY FL C_5-ceramide complexed to BSA (5 μM, 30 min, λ_{ex} = 488 nm, λ_{em} = 500 – 550 nm) in HBSS at 4°C. After washing with ice-cold HBSS (1 mL × 3), the cells were further incubated in fresh HBSS at 37°C under a 5% CO_2 atmosphere for 30 min. The PCCs were determined using the program ImageJ (Version 1.4.3.67).

For imaging of furin activity, HeLa cells were incubated with conjugate **1a-FC-QSY7** (10 μM, 6 h), washed with PBS (1 mL × 3) and then imaged using a Leica TCS SPE. For the control experiment, HeLa cells were pretreated with the furin inhibitor (500 μM, 30 min), washed with PBS (1 mL × 3), followed by incubation with conjugate **1a-FC-QSY7** (10 μM, 6 h). After washing with PBS (1 mL × 3), the cells were imaged using a Leica TCS SPE.

MTT Assays

HeLa and HEK 293 cells were seeded in a 96-well flat-bottomed microplate (*ca.* 10,000 cells per well) in a growth medium (100 μL) and incubated at 37°C under a 5% CO_2

atmosphere for 48 h. The growth medium was removed and replaced with the conjugates of complex **1a** in growth medium/DMSO (99:1, *v*/*v*) at 37°C under a 5% CO_2 atmosphere for 24 h. After treatment, the medium was removed and replenished with phenol red-free growth medium (100 μL). One of the microplates was kept in the dark for 10 min, while the other microplate was irradiated with an LED (450 nm, 10 mW cm^{-2}, 10 min) cellular photocytotoxicity irradiator (PURI Materials, Shenzhen, China). The growth medium was replaced with fresh DMEM (100 μL) and the cells were further incubated at 37°C under a 5% CO_2 atmosphere for 24 h. After replenished with fresh DMEM (90 μL) and a solution of MTT in PBS (10 μL, 5 mg mL^{-1}), the cells were incubated at 37°C under a 5% CO_2 atmosphere for 4 h. The growth medium was removed and DMSO (100 μL) was added to each well. The microplates were further incubated at 37°C under a 5% CO_2 atmosphere for 15 min. The absorbance of the solutions at 570 nm was measured with a SPECTRAmax 340 microplate reader (Molecular Devices Corp., Sunnyvale, CA).

Studies of the Cell Death Mechanism

The intracellular ROS levels were assessed by using a fluorogenic probe CM-H_2DCFDA,[10] the cytoplasmic membrane was stained by CellMask Deep Red,[11] the nucleus morphology was visualised by staining with Hoechst 33342[12] and MMP was analysed using Rhodamine 123 as the indicator.[13] HeLa cells in growth medium were seeded on a sterilised coverslip in 35-mm tissue culture dishes and grown at 37°C under a 5% CO_2 atmosphere for 48 h. The culture medium was removed and replaced with conjugate **1a-FC-QSY7** (10 μM, 4 h, λ_{ex} = 405 nm) in DMEM/DMSO (99:1, *v*/*v*) at 37°C under a 5% CO_2 atmosphere. The cells were washed with PBS (1 mL × 3) and

replenished by phenol red-free medium. The tissue culture dish was kept in the dark for 10 min or irradiated at 450 nm (10 mW cm^{-2}, 10 min) with an LED cellular photocytotoxicity irradiator (PURI Materials, Shenzhen, China). The cells were washed with PBS (1 mL × 3) and subsequently stained with CM-H_2DCFDA (5 μM, 30 min; λ_{ex} = 488 nm, λ_{em} = 500 – 550 nm), CellMask Deep Red (5 μM, 15 min; λ_{ex} = 635 nm, λ_{em} = 650 – 700 nm), Hoechst 33342 (5 μM, 15 min; λ_{ex} = 405 nm, λ_{em} = 415 – 495 nm), Rhodamine 123 (5 μM, 15 min; λ_{ex} = 488 nm, λ_{em} = 500 − 550 nm) or CellEvent Caspase-3/7 Red (20 μL, 1:100, 1 h, λ_{ex} = 590 nm, λ_{em} = 610 − 630 nm) in DMEM at 37°C under a 5% CO_2 atmosphere. The cells were washed with PBS (1 mL × 3) and then mounted onto a sterilised glass slide for imaging.

Annexin V/PI Assays

HeLa cells in growth medium were seeded on two 6-well plates and grown at 37°C under a 5% CO_2 atmosphere for 48 h. HeLa cells were treated without or with conjugate **1a-FC-QSY7** (5 μM, 24 h) in DMEM/DMSO (99:1, *v*/*v*) at 37°C under a 5% CO_2 atmosphere. The cells were washed with PBS (1 mL × 3) and fresh phenol red-free medium was added. The cells were kept in the dark for 10 min or photoirradiated at 450 nm (10 mW cm^{-2}, 10 min). After further incubation in fresh DMEM (100 μL) at 37°C under a 5% CO_2 atmosphere for 4 h, the medium was removed, followed by washing with PBS (1 mL × 3). The cells were then trypsinised and centrifuged at 1500 rpm for 1 min and the resulting cell pellet was washed with PBS (1 mL) and subjected to centrifugation. The cells were resuspended in an Annexin-V binding buffer (100 μL) in the flow cytometer tubes, followed by the addition of the PI (100 μg mL^{-1}, 15 min, 15 min, λ_{ex} = 561 nm) and Alexa Fluor 647-Annexin V conjugate (5 μL, 50 μL mL^{-1}, 15

min, λ_{ex} = 638 nm). The cell suspension was kept in the dark for 15 min, followed by the addition of Annexin V binding buffer (400 μL) and was analysed by flow cytometer (Beckman CytoFLEX). The cells without any treatment were used as a control group for background correction. The experiments were performed in triplicates and analysed using the FlowJo V10 software.

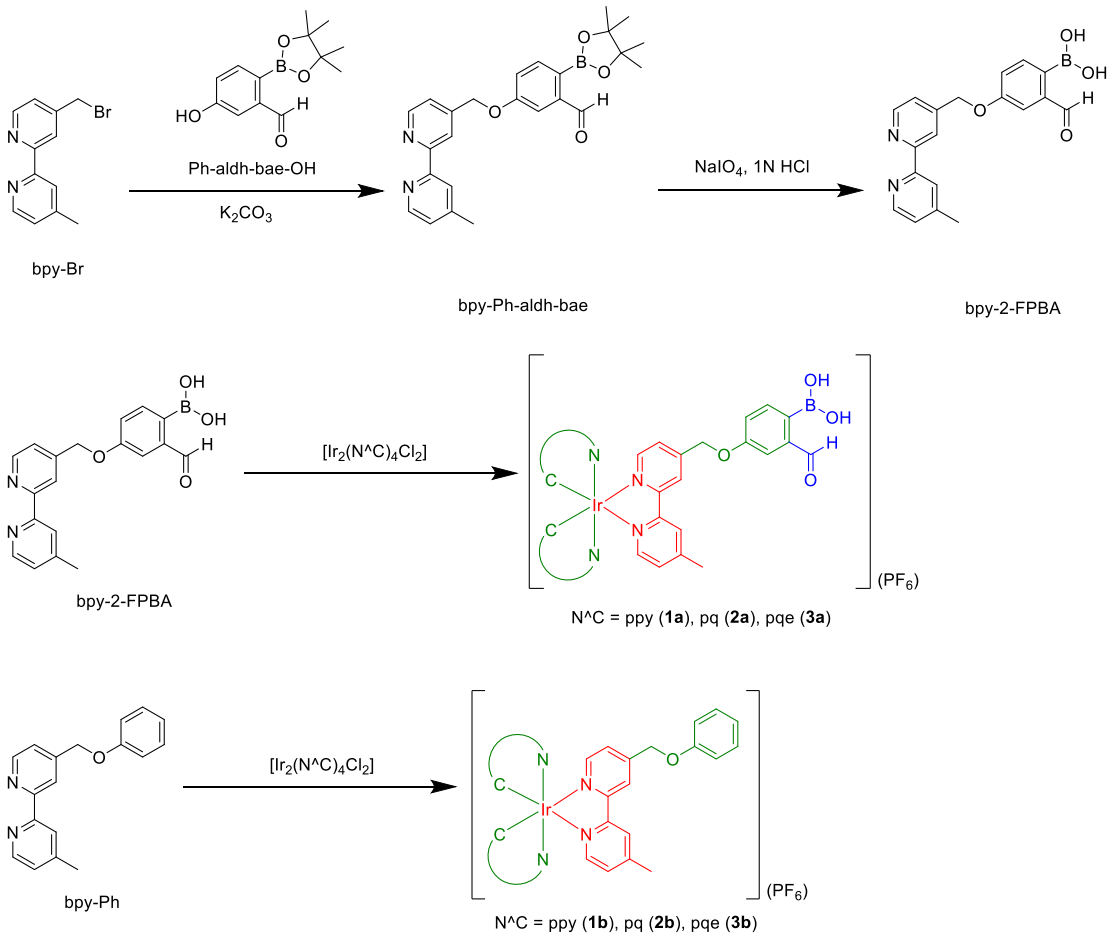

Scheme S1 Synthetic routes of the ligands and complexes.

Table S1 Electronic absorption spectral data of complexes **1a** – **3a** and **1b** – **3b** in CH_2Cl_2 and CH_3CN at 298 K.

Complex	Solvent	λ_{abs}/nm (ε/dm^3 mol^{-1} cm^{-1})
1a	CH_2Cl_2	257 (58,950), 311 sh (24,470), 339 sh (10,585), 380 (7,395), 417 sh (3,890), 480 (985)
	CH_3CN	255 (57,095), 309 sh (23,960), 338 (11,670), 378 (6,130), 414 sh (3,470), 482 (940)
1b	CH_2Cl_2	259 (61,130), 270 sh (58,345), 310 sh (25,970), 337 sh (11,790), 382 (8,085), 415 sh (4,330), 480 (990)
	CH_3CN	255 (59,275), 267 (56,440), 309 (25,260), 337 sh (11,435), 379 (6,160), 413 sh (4,115), 482 (945)
2a	CH_2Cl_2	266 (73,020), 281 sh (70,140), 334 (31,875), 441 (6,280)
	CH_3CN	260 (72,270), 280 sh (65,210), 336 (29,610), 430 (6,215)
2b	CH_2Cl_2	278 (70,470), 308 sh (31,610), 339 (31,275), 441 (6,150)
	CH_3CN	271 (68,640), 301 sh (31,085), 337 (29,905), 438 (6,810)
3a	CH_2Cl_2	266 (67,550), 292 (61,190), 356 sh (31,590), 462 (4,950)
	CH_3CN	262 (69,105), 262 (69,105), 349 sh (31,260), 458 (5,140)
3b	CH_2Cl_2	268 (64,950), 292 (61,245), 354 sh (32,835), 472 (5,125)
	CH_3CN	267 (64,770), 290 (58,970), 352 sh (31,480), 461 (5,890)

Table S2 Photophysical data of complexes **1a** – **3a** and **1b** – **3b**.

Complex	Medium (*T*/K)	λ_{em}/nm[a]	τ_o/μs[b]	Φ_{em}[c]
1a	CH_2Cl_2 (298)	575	0.61	0.24
	CH_3CN (298)	586	0.36	0.10
	Buffer/MeOH[d] (298)	590	0.15	0.07
	Glass[e] (77)	515, 536 sh	4.33	
1b	CH_2Cl_2 (298)	578	0.62	0.32
	CH_3CN (298)	590	0.35	0.20
	Buffer/MeOH[d] (298)	590	0.14	0.08
	Glass[e] (77)	515, 533 sh	4.58	
2a	CH_2Cl_2 (298)	557	2.36	0.65
	CH_3CN (298)	560	1.77	0.47
	Buffer/MeOH[d] (298)	557	1.09	0.50
	Glass[e] (77)	543 (max), 582, 639 sh	4.72	
2b	CH_2Cl_2 (298)	556	2.51	0.61
	CH_3CN (298)	558	1.98	0.43
	Buffer/MeOH[d] (298)	557	1.06	0.45
	Glass[e] (77)	542 (max), 582, 638 sh	4.70	
3a	CH_2Cl_2 (298)	622	1.22	0.26
	CH_3CN (298)	640	0.63	0.12
	Buffer/MeOH[d] (298)	655	0.04	0.007
	Glass[e] (77)	597, 648 sh	4.89	
3b	CH_2Cl_2 (298)	623	1.42	0.22

CH_3CN (298)	639	0.74	0.13
Buffer/MeOH[d] (298)	655	0.04	0.007
Glass[e] (77)	598, 648 sh	4.82	

[a] λ_{ex} = 350 nm.

[b] The lifetimes were measured at the emission maxima (λ_{ex} = 355 nm).

[c] $[Ru(bpy)_3]Cl_2$ was used as a reference (Φ_{em} = 0.040 in aerated H_2O, λ_{ex} = 455 nm).[7]

[d] Potassium phosphate buffer (50 mM, pH 7.4)/MeOH (1:1, *v*/*v*).

[e] EtOH/MeOH (4:1, *v*/*v*)

Table S3 The $^1O_2$ generation quantum yields of complexes **1a** – **3a** and **1b** – **3b** in aerated MeOH at 298 K.

Complex	Φ_Δ[a]
1a	0.77
1b	0.79
2a	0.83
2b	0.86
3a	0.72
3b	0.75

[a] $[Ru(bpy)_3]Cl_2$ was used as the reference (Φ_Δ = 0.73 in aerated MeOH).[9]

Table S4 Photophysical data of the conjugates of complex **1a** in degassed KPi (50 mM, pH 7.4)/MeOH (1:1, *v*/*v*).

Conjugate	λ_{em}/nm[a]	τ_o/μs[b]	Φ_{em}[c]
1a-Cys	592	0.14	0.08
1a-ER	592	0.15	0.08
1a-GA	592	0.16	0.07
1a-FC	592	0.15	0.08
1a-FC-QSY7	610	0.04	0.003

[a] λ_{ex} = 350 nm.

[b] The lifetimes were measured at the emission maxima (λ_{ex} = 355 nm).

[c] $[Ru(bpy)_3]Cl_2$ was used as a reference (Φ_{em} = 0.040 in aerated H_2O, λ_{ex} = 455 nm).[7]

Table S5 The $^1O_2$ generation quantum yields of the conjugates of complex **1a** in aerated MeOH at 298 K.

Complex	Φ_Δ[a]
1a-Cys	0.75
1a-ER	0.74
1a-GA	0.73
1a-FC	0.72
1a-FC-QSY7	0.51

[a] $[Ru(bpy)_3]Cl_2$ was used as the reference (Φ_Δ = 0.73 in aerated MeOH).[9]

Table S6 (Photo)cytotoxicity (IC_{50}, μM) of the conjugates of complex **1a** toward HeLa and HEK 293 cells under dark or light conditions (λ_{ex} = 450 nm, 10 mW cm^{-2}, 10 min).

	HeLa			HEK 293			
Conjugate	$IC_{50,dark}$	$IC_{50,light}$	PI[a]	$IC_{50,dark}$	$IC_{50,light}$	PI[a]	SI[b]
1a-Cys	28.0 ± 2.2	1.1 ± 0.1	25	29.0 ± 0.2	2.9 ± 0.1	10	3
1a-ER	26.1 ± 0.9	2.6 ± 0.1	10	33.7 ± 0.3	3.3 ± 0.1	10	1
1a-GA	33.7 ± 0.2	5.2 ± 0.4	6	38.7 ± 1.2	6.3 ± 0.2	6	1
1a-FC-QSY7	29.1 ± 2.4	1.3 ± 0.1	22	31.5 ± 0.5	8.2 ± 0.1	4	6

[a] Photocytotoxicity Index (PI) = $IC_{50,dark}/IC_{50,light}$.

[b] Cancer Selectivity Index (SI) = $IC_{50,light}$ (HeLa)/$IC_{50,light}$ (HEK 293).

Table S7 Cellular uptake of the conjugates of complex **1a** towards HeLa and HEK 293 cells.

	Amount of iridium per cell/fmol[a]	
Conjugate	HeLa	HEK293
1a-Cys	0.26 ± 0.04	0.16 ± 0.01
1a-ER	0.23 ± 0.06	0.14 ± 0.04
1a-GA	0.20 ± 0.01	0.10 ± 0.01
1a-FC-QSY7	1.08 ± 0.06	0.43 ± 0.02

[a] Amount of iridium associated with an average cell upon incubation with the conjugates (10 μM) at 37°C for 4 h, as determined by ICP-MS.

Table S8 FRET parameters of conjugate **1a-FC-QSY7**.

Donor	Acceptor	$J(\lambda)^a$/nm^4 M^{-1} cm^{-1}	R_o/ Å	d^b/Å	E_{calc}	E_{expt}
1a-FC	QSY7	4.01 x 10^{17}	88.5	29.8	0.99	0.97

[a] Overlap integral of the emission spectrum of the QSY7-free conjugate **1a-FC** and the absorption spectrum of QSY7 (acceptor).

[b] Distance between the iridium(III) atom and QSY7 in **1a-FC-QSY7**.

Fig. S1 Electronic absorption spectra of complexes **1a** – **3a** and **1b** – **3b** in CH_2Cl_2 (black) and CH_3CN (red) at 298 K.

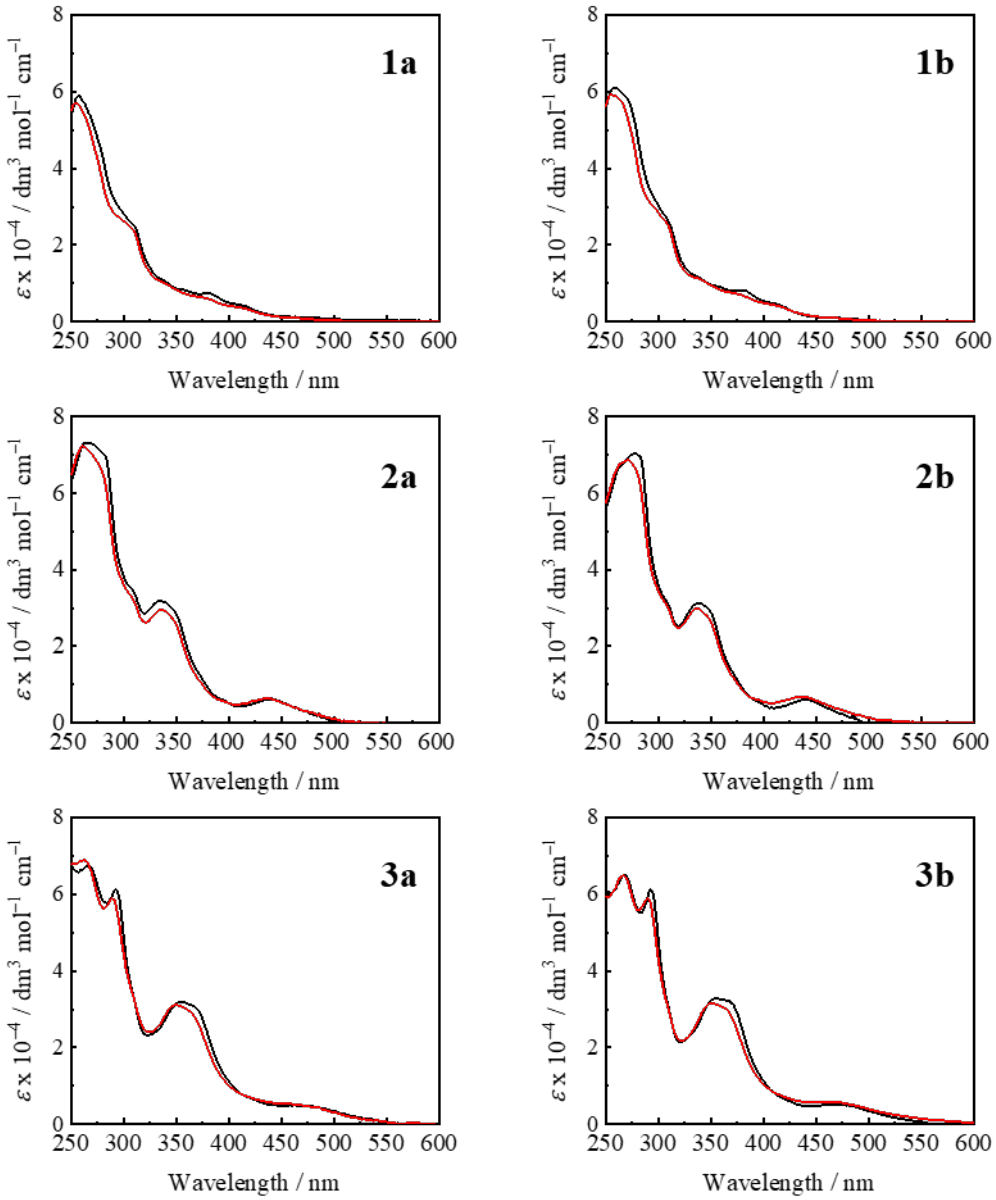

Fig. S2 Normalised emission spectra of complexes **1a** – **3a** and **1b** – **3b** in CH_2Cl_2 (black) and CH_3CN (red) at 298 K and alcohol glass at 77 K (blue).

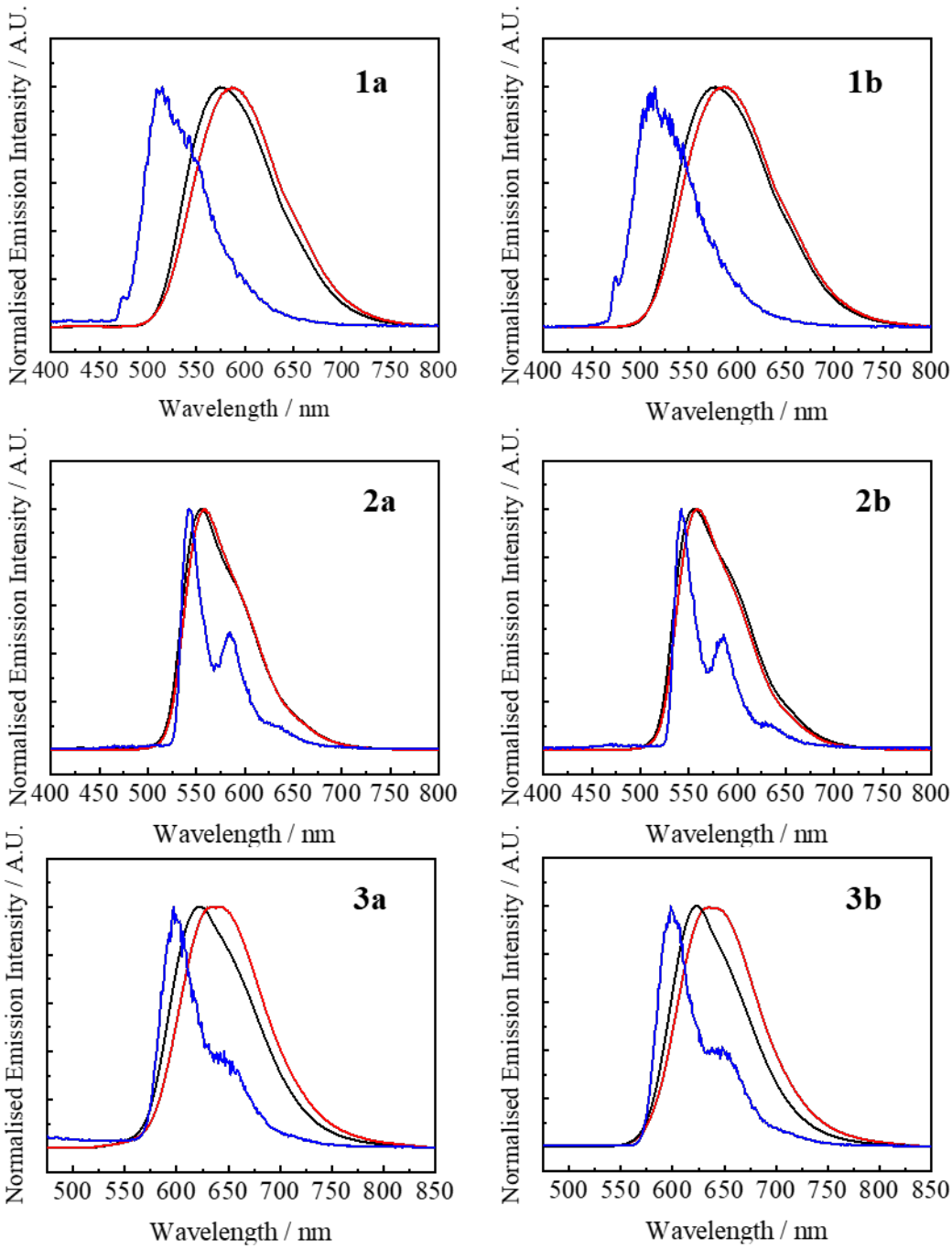

Fig. S3 HPLC chromatograms of the reaction mixtures of complexes (a) **1a** (25 μM), (b) **2a** (25 μM) and (c) **3a** (25 μM) without (black) or with L-Cys (100 μM) (red) in ammonium acetate buffer (50 mM, pH 7.4)/DMF (9:1, *v*/*v*) containing TCEP (400 μM) after incubation at 37°C for 4 h. The absorbance was monitored at 210 nm.

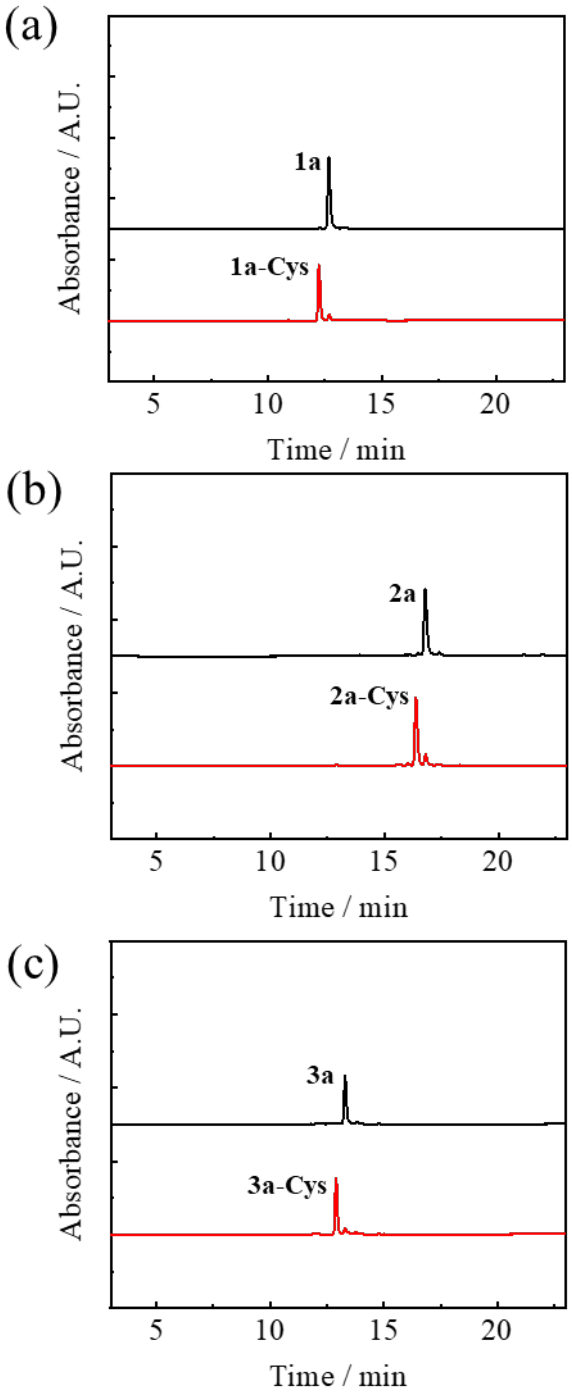

Fig. S4 ESI-mass spectra of the reaction mixtures of complexes (a) **1a** (25 μM), (b) **2a** (25 μM) and (c) **3a** (25 μM) with L-Cys (100 μM) in ammonium acetate buffer (50 mM, pH 7.4)/DMF (9:1, *v*/*v*) containing TCEP (400 μM) after incubation at 37°C for 4 h.

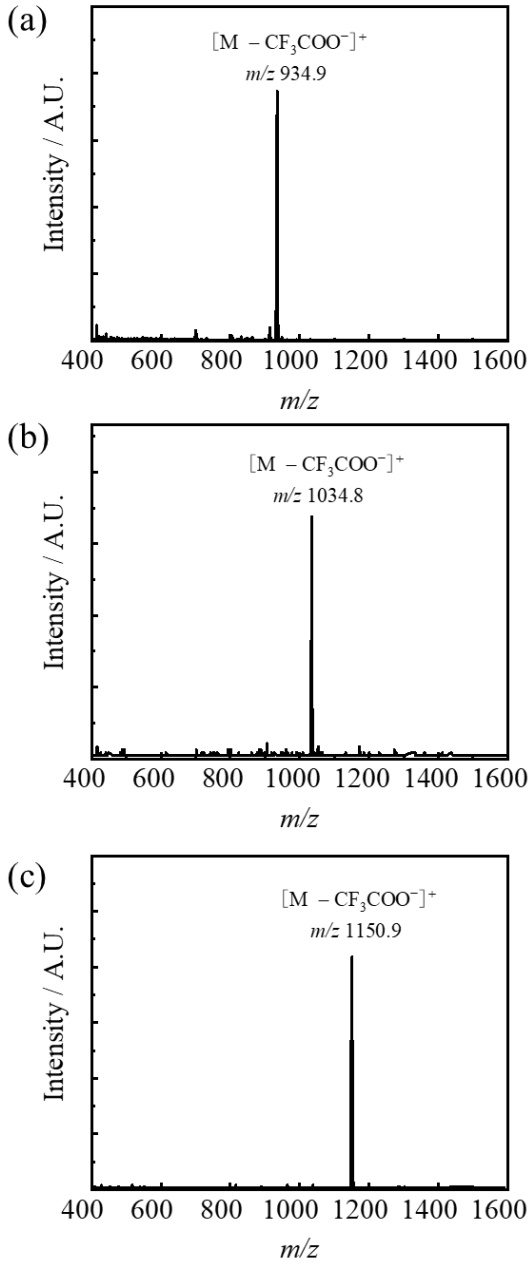

Fig. S5 Second-order kinetics for the reaction of (a)complex **1** (25 μM), (b) complex **2** (25 μM) and (c) complex **3** (25 μM) with L-Cys (125 μM) at different time points in ammonium acetate buffer (50 mM, pH 7.4)/DMF (9:1, *v*/*v*) containing TCEP (500 μM) after incubation at 37°C. The slope of the linear fit corresponds to the k_2 of the reaction.

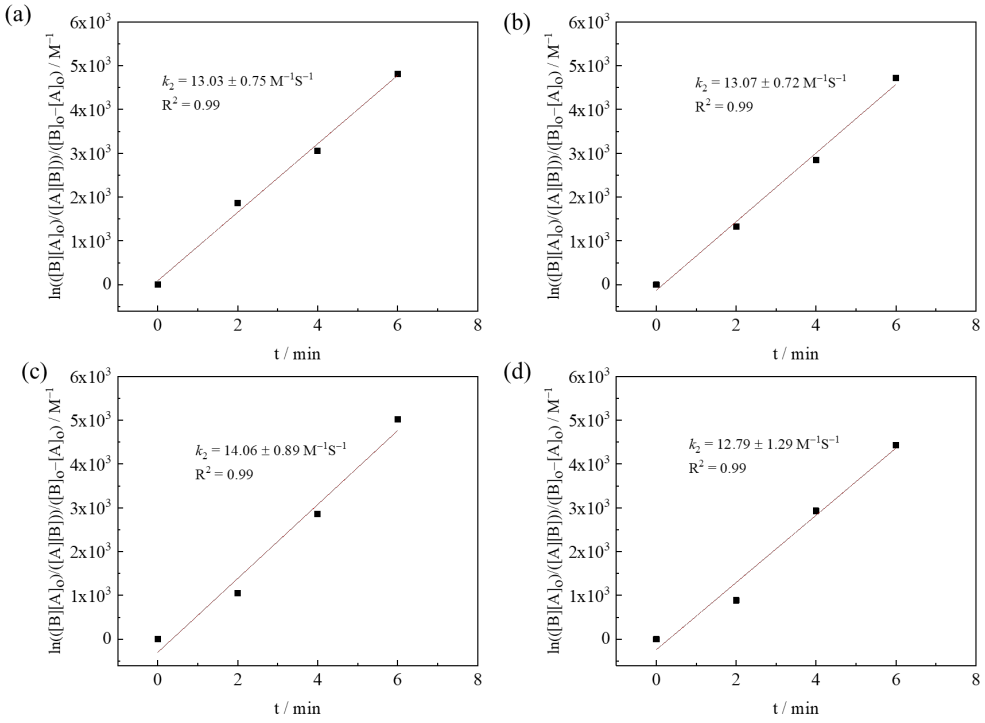

Fig. S6 HPLC chromatograms of (a) complex **1** (25 μM), (b) complex **2** (25 μM) and (c) complex **3** (25 μM) after incubation in ammonium acetate buffer (50 mM, pH 7.5)/DMF (9:1, *v*/*v*) at 37°C for 0 and 12 h. The absorbance was monitored at 350 nm.

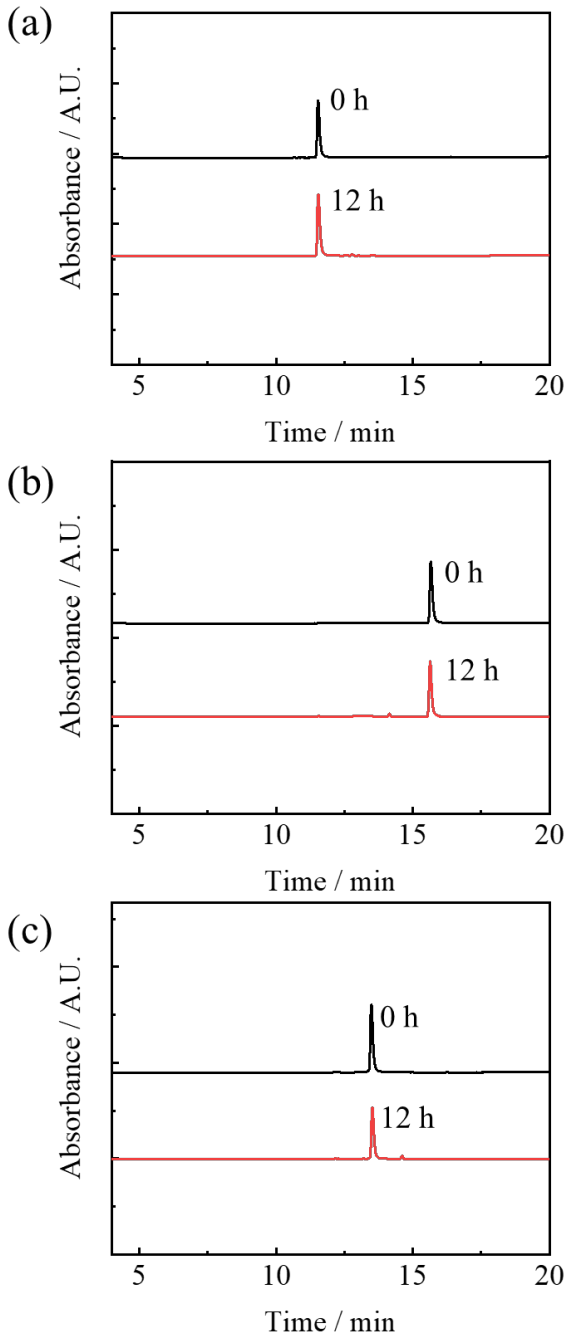

Fig. S7 (a) HPLC chromatograms of the reaction mixture of complex **1a** (25 μM) without (black) or with L-Cys (100 μM), L-Lys (100 μM), L-Met (100 μM) and L-Ser (100 μM) (red) in ammonium acetate buffer (50 mM, pH 7.4)/DMF (9:1, *v*/*v*) containing TCEP (400 μM) after incubation at 37°C for 4 h. The absorbance was monitored at 350 nm. (b) ESI-mass spectrum of the new emerging peak collected from HPLC eluent at t_R = 12.6 min.

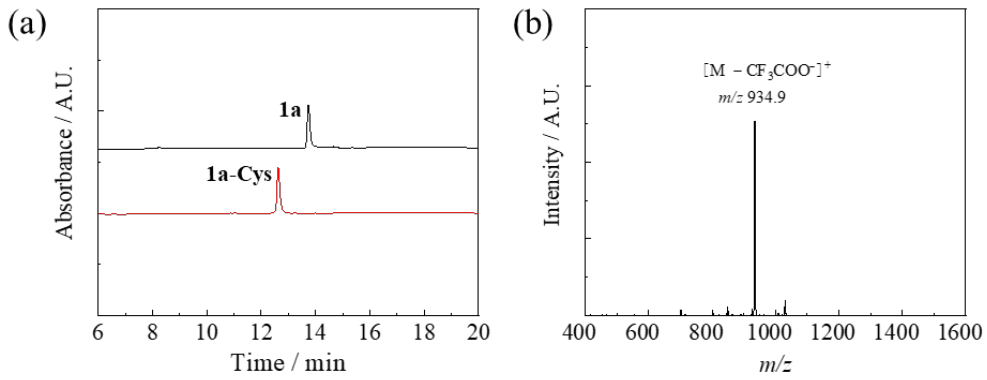

Fig. S8 HPLC chromatograms of (a) complex **1a** (25 μM) and (b) the reaction mixture of complex **1a** (25 μM) and CKDEL (100 μM) in ammonium acetate buffer (50 mM, pH 7.4)/DMF (9:1, *v*/*v*) containing TCEP (400 μM) after incubation at 37°C for 4 h. The absorbance was monitored at 210 nm.

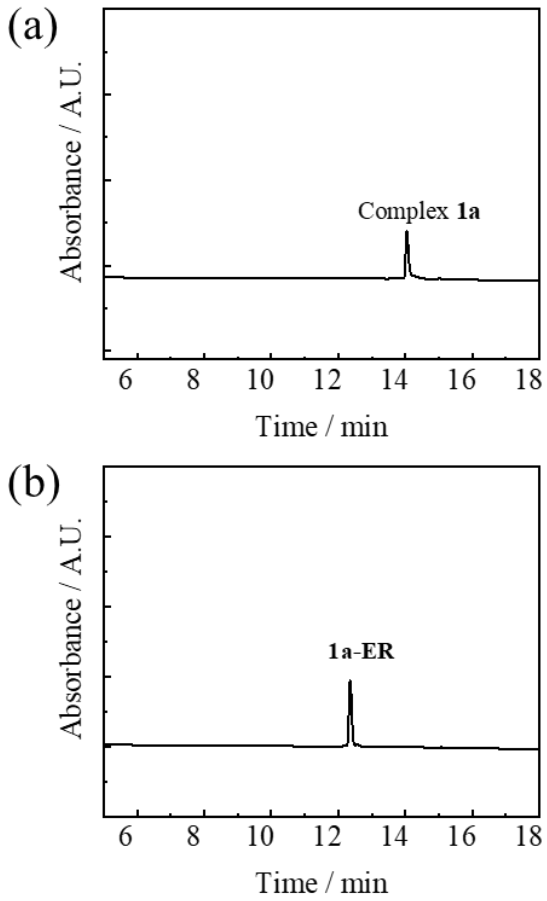

Fig. S9 HPLC chromatograms of (a) complex **1a** (25 μM), (b) CSDYQRL (100 μM) and (c) a reaction mixture of complex **1a** (25 μM) and CSDYQRL (100 μM) in ammonium acetate buffer (50 mM, pH 7.4)/DMF (9:1, *v*/*v*) containing TCEP (400 μM) after incubation at 37°C for 4 h. The absorbance was monitored at 210 nm.

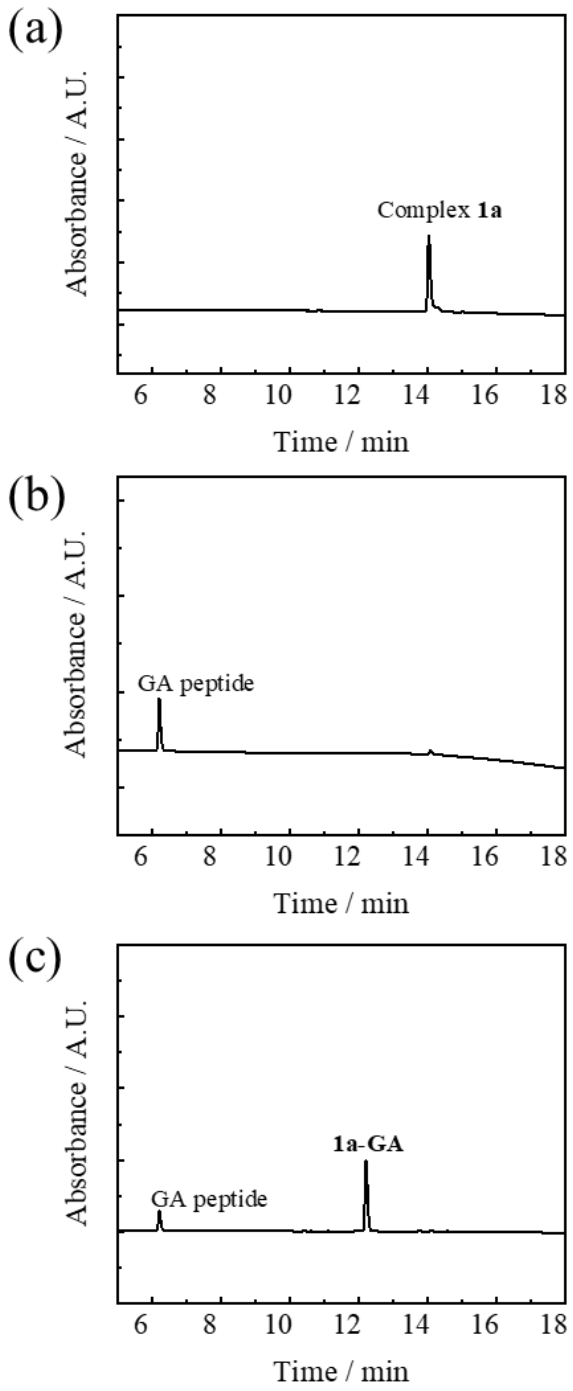

Fig. S10 HPLC chromatograms of the purified conjugates **1a-Cys**, **1a-ER** and **1a-GA**. The absorbance was monitored at 350 nm.

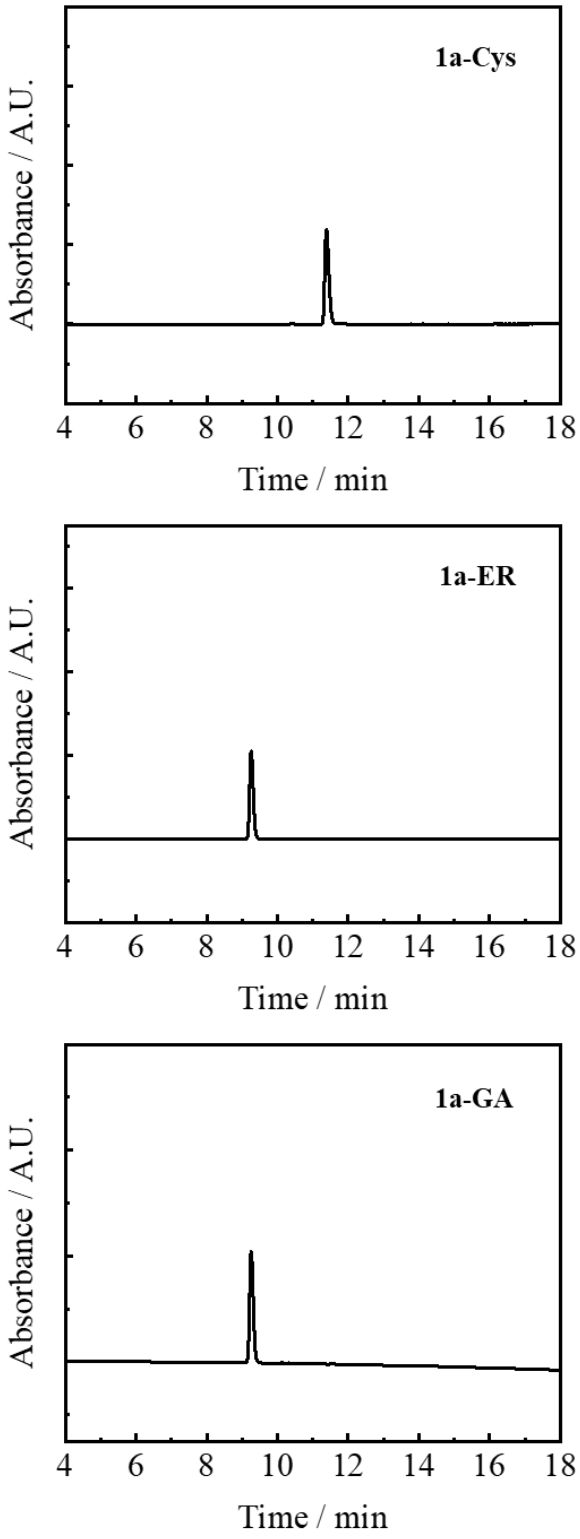

Fig. S11 ESI-mass spectra of the purified conjugates **1a-Cys**, **1a-ER** and **1a-GA**.

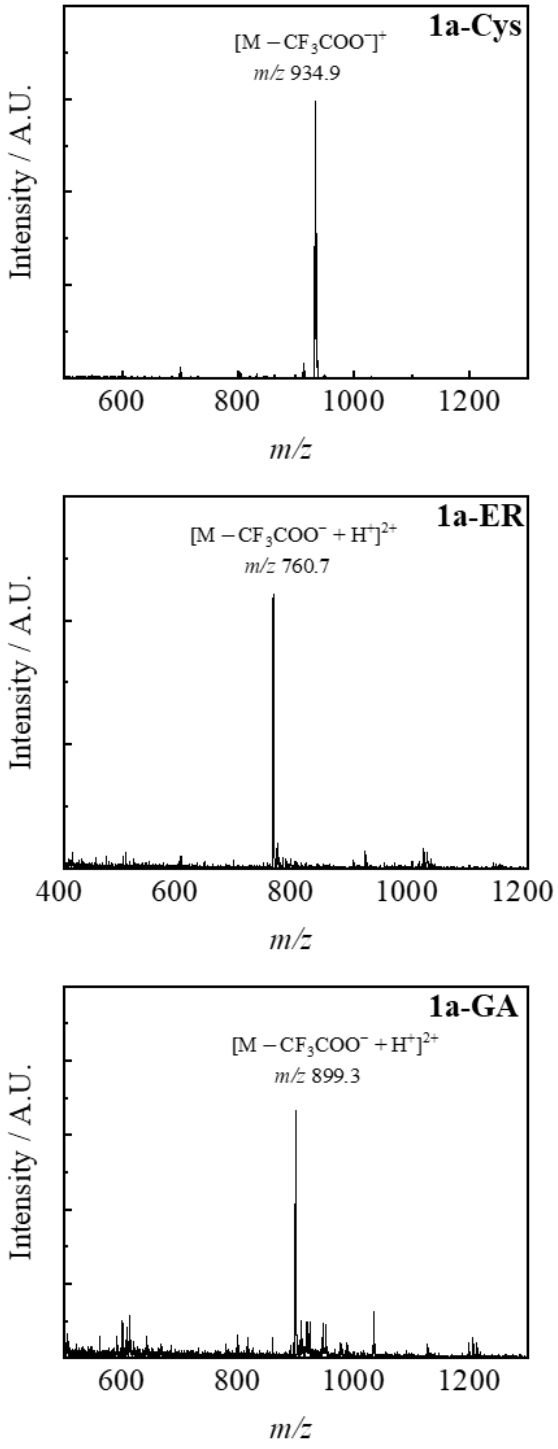

Fig. S12 LSCM images of HeLa cells incubated with (a) conjugate **1a-Cys** (20 μM, 4 h, λ_{ex} = 405 nm, λ_{em} = 550 – 650 nm), (b) **1a-ER** (20 μM, 4 h, λ_{ex} = 405 nm, λ_{em} = 550 – 650 nm) or (c) **1a-GA** (20 μM, 16 h, λ_{ex} = 405 nm, λ_{em} = 550 – 650 nm), and then LysoTracker Deep Red (100 nM, 30 min, λ_{ex} = 635 nm, λ_{em} = 650 – 680 nm), LysoTracker Green (100 nM, 30 min, λ_{ex} = 488 nm, λ_{em} = 500 – 550 nm) or MitoTracker Green (100 nM, 20 min, λ_{ex} = 488 nm, λ_{em} = 500 – 550 nm), respectively. Scale bar = 20 μm.

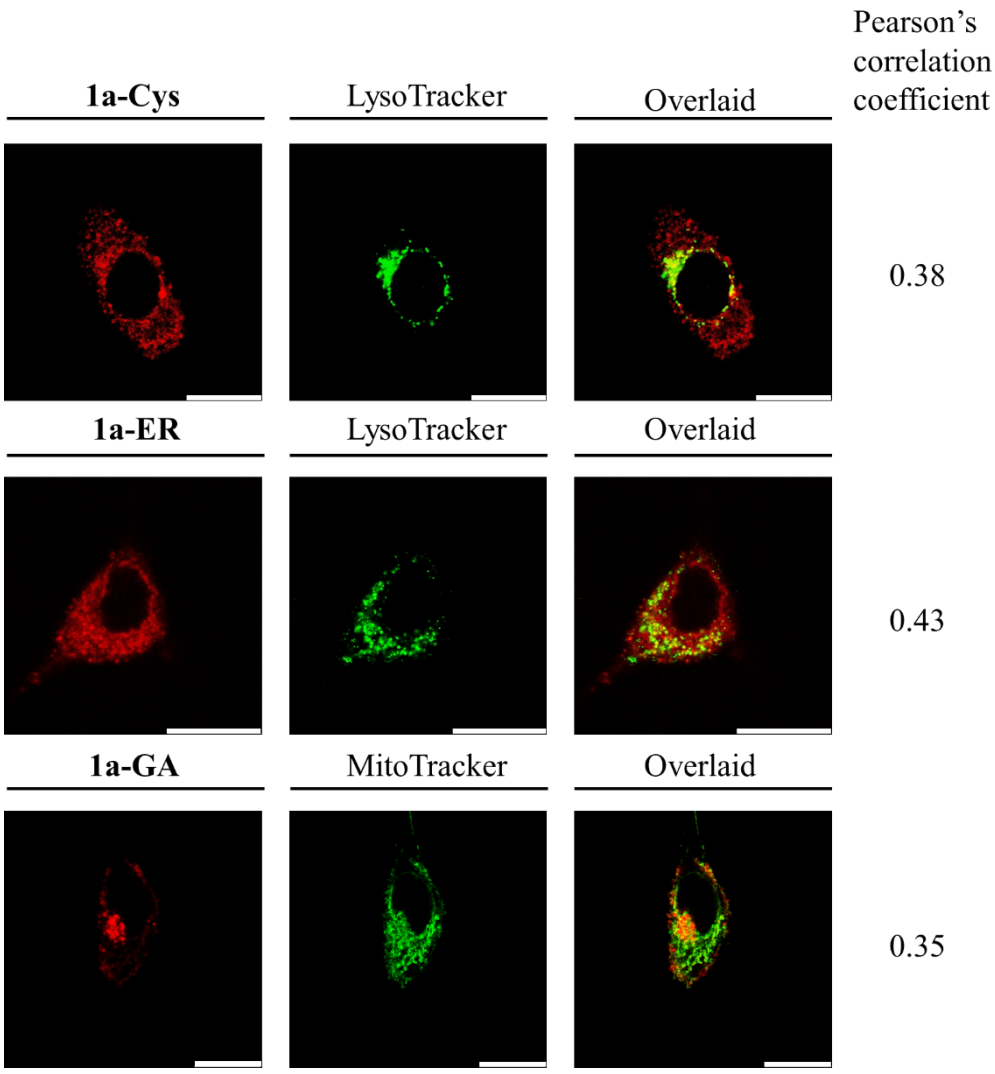

Fig. S13 HPLC chromatograms of (a) complex **1a** (25 μM), (b) CGGGGRVRRSVK (FC) (100 μM) and (c) a reaction mixture of complex **1a** (25 μM) and FC peptide (100 μM) in ammonium acetate buffer (50 mM, pH 7.4)/DMF (9:1, *v*/*v*) containing TCEP (400 μM) after incubation at 37°C for 4 h. The absorbance was monitored at 210 nm. (d) ESI-mass spectrum of the purified conjugate **1a-FC**.

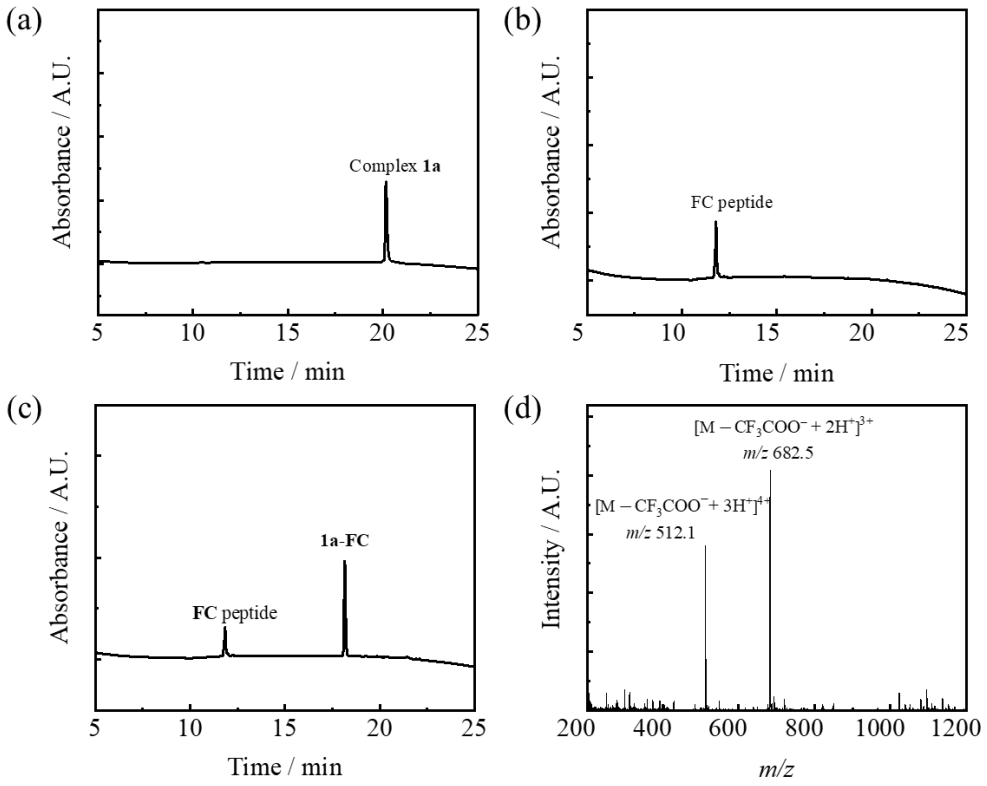

Fig. S14 ESI-mass spectra of the conjugates (a) **1a-CGGGGRVRR** and (b) **SVK-QSY7** collected from the HPLC eluent at t_R = 9.3 and t_R = 10.3 min, respectively.

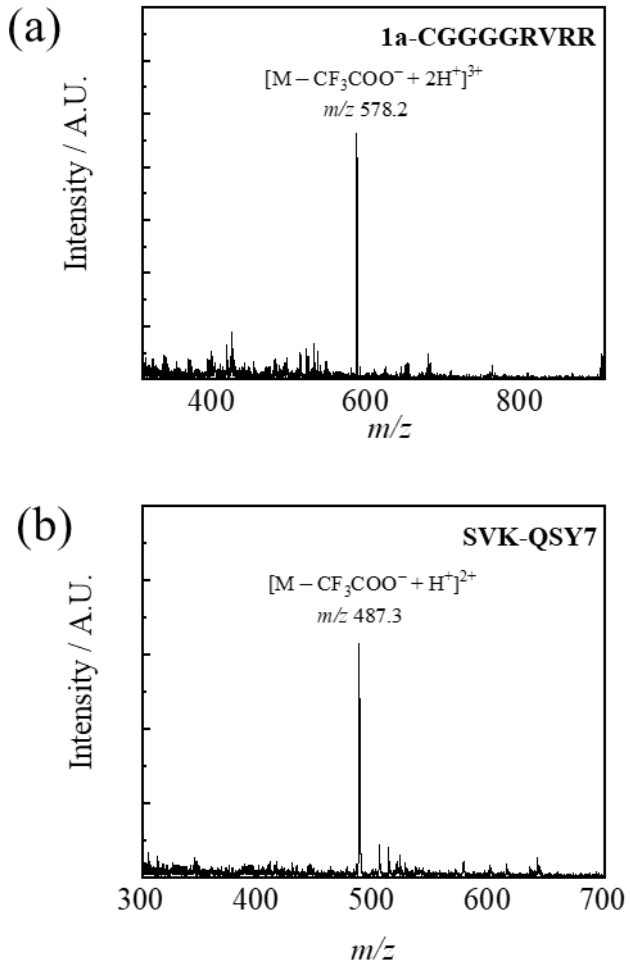

Fig. S15 LSCM images of caspase 3/7 activity of HeLa cells upon pretreatment with conjugate **1a-FC-QSY7** (10 μM, 4 h) without (left) or with (right) light irradiation (450 nm, 10 mW cm^{-2}, 10 min) and further incubation with CellEvent Caspase-3/7 Red (20 μL, 1:100, 1 h, λ_{ex} = 590 nm, λ_{em} = 610 – 630 nm).

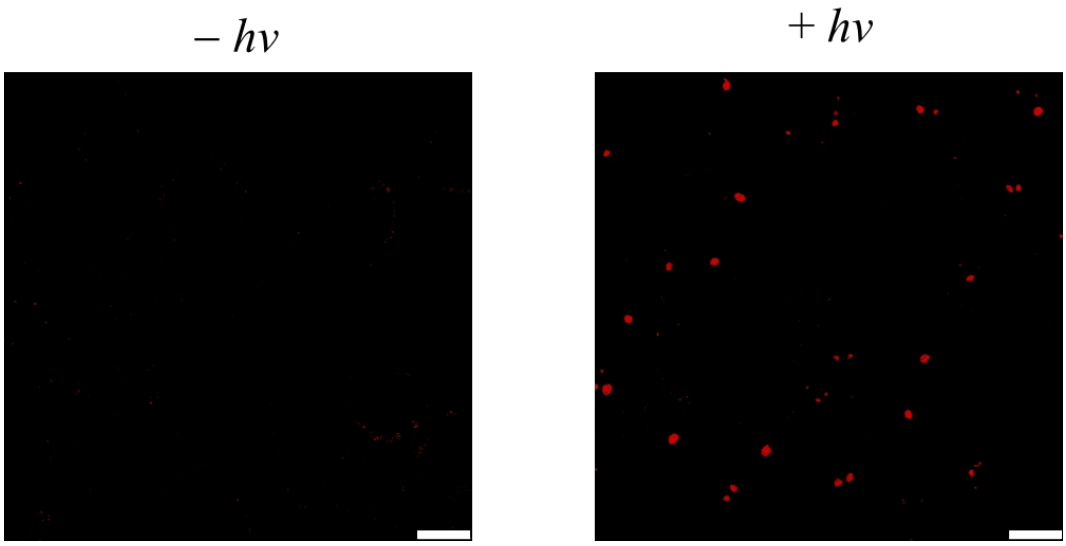

Fig. S16 Flow cytometric analysis of HeLa cells treated without (a) or with conjugate **1a-FC-QSY7** (5 μM) in the dark for 24 h, then washed thoroughly with PBS, incubated in the dark (b) or irradiated at 450 nm (10 mW cm^{-2}) (c) for 10 min and subsequently incubated in the dark for 4 h. They were then stained with PI (100 μg mL^{-1}, 15 min, λ_{ex} = 561 nm) and Alexa Fluor 647-Annexin V conjugate (50 μL mL^{-1}, 15 min, λ_{ex} = 638 nm).

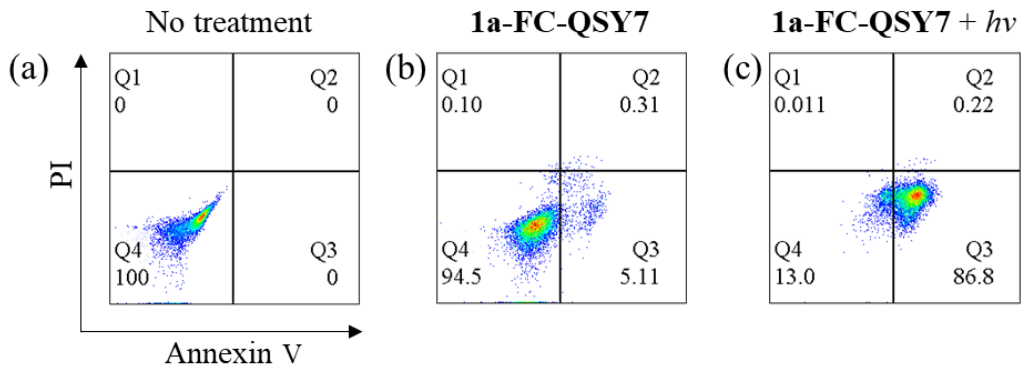

Fig. S17 ^{1}H NMR spectrum of bpy-Ph-aldh-bae in $CDCl_3$ at 298 K.

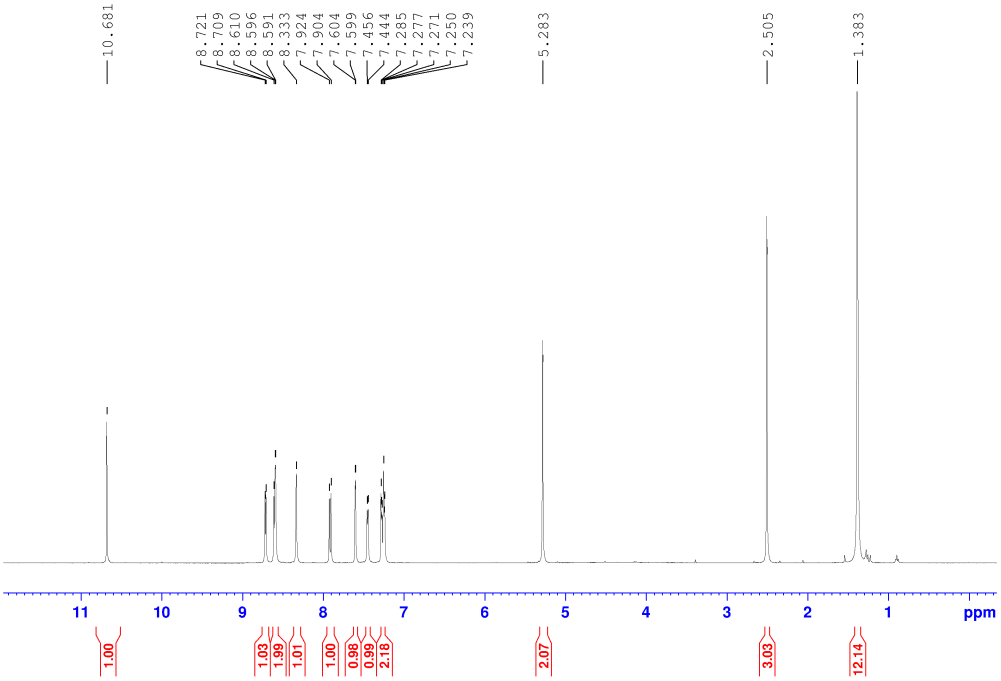

Fig. S18 ^{1}H NMR spectrum of bpy-2-FPBA in DMSO-d_6 at 298 K.

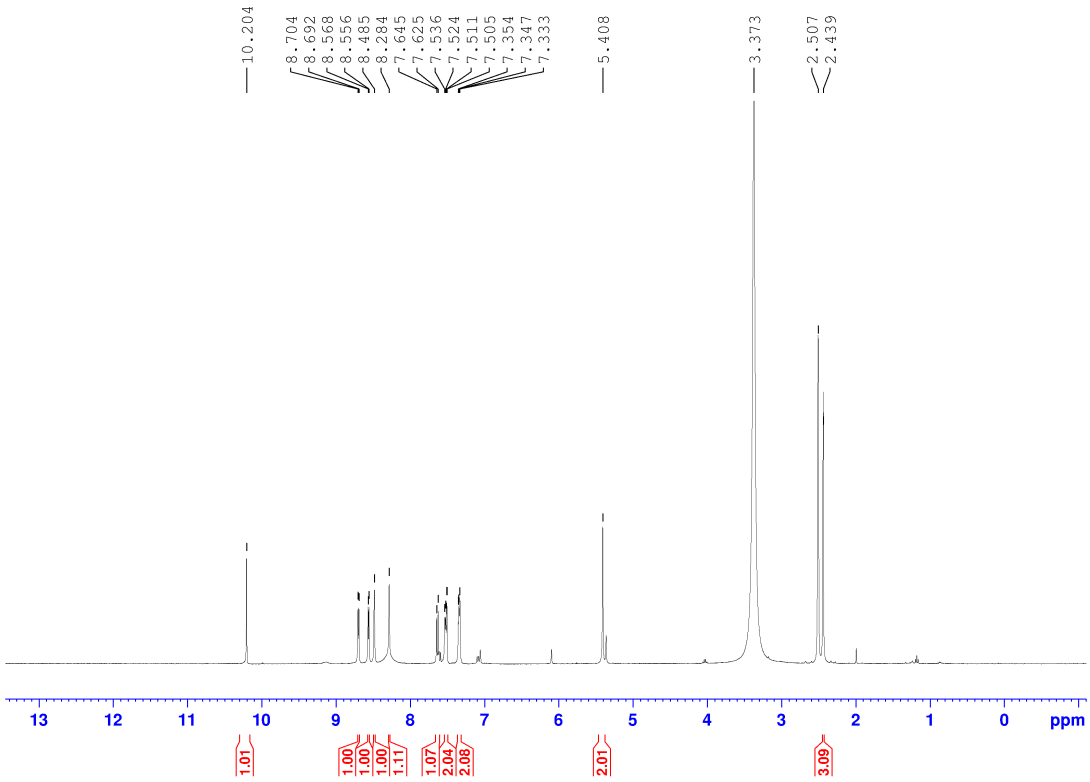

Fig. S19 ^{1}H NMR spectrum of complex **1a** in DMSO-d_6 at 298 K.

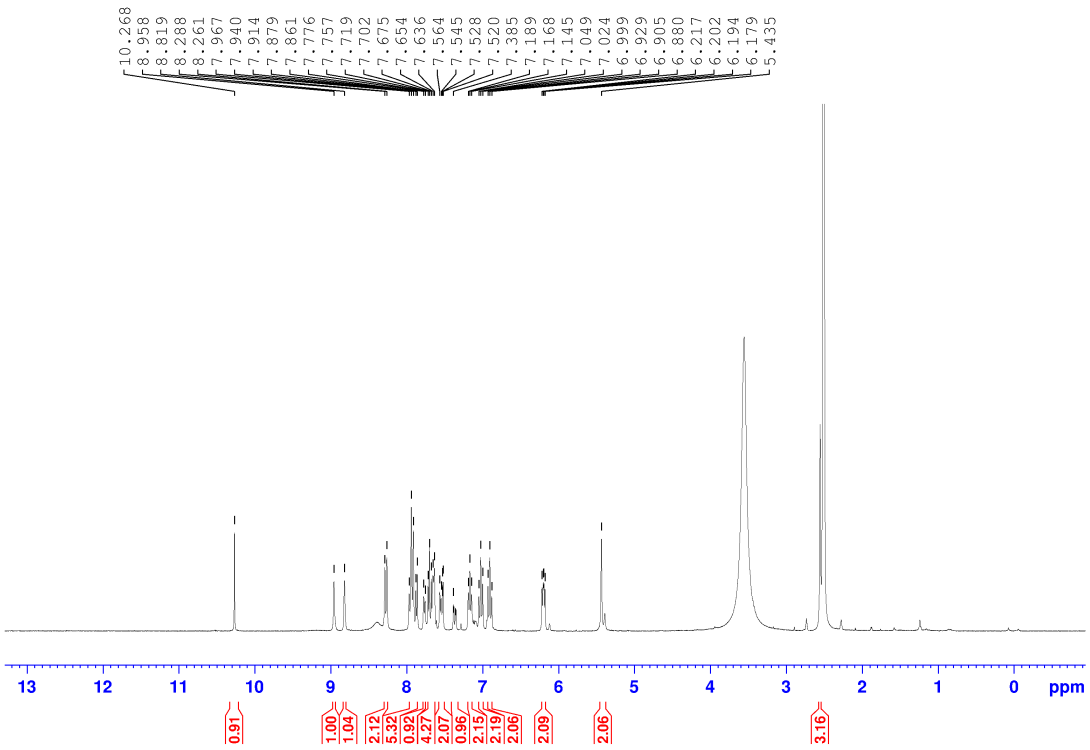

Fig. S20 ^{13}C NMR spectrum of complex **1a** in DMSO-d_6 at 298 K.

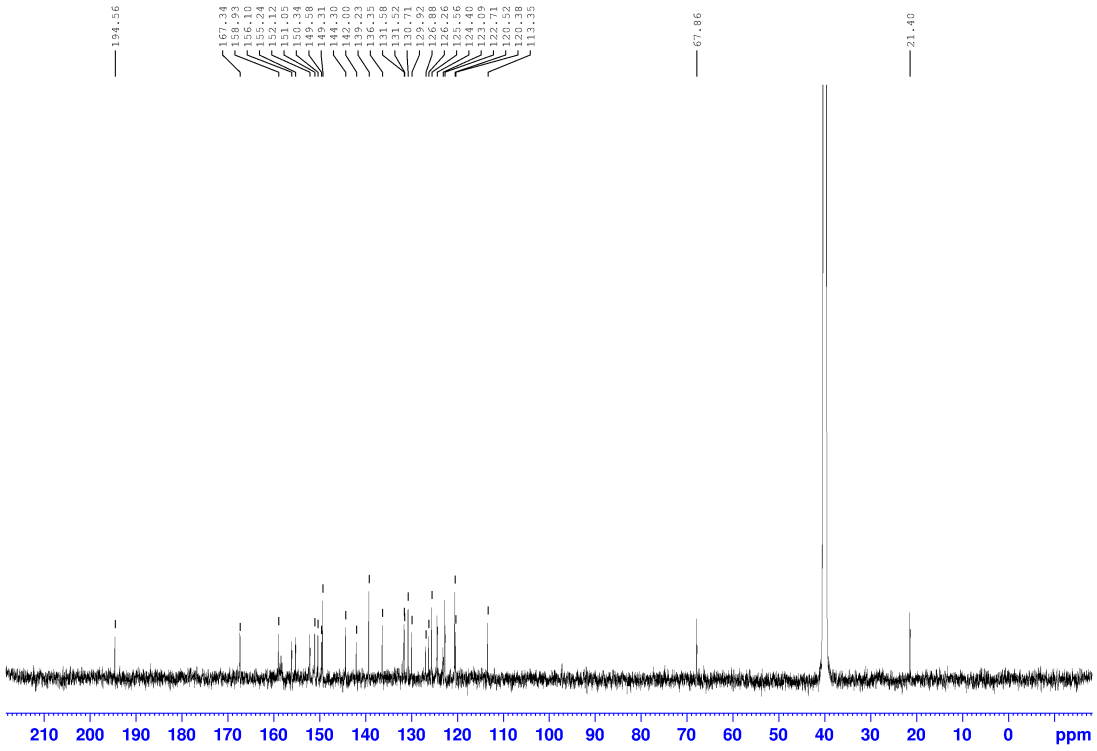

Fig. S21 HR-ESI-mass spectra of complex **1a** in CH_3CN.

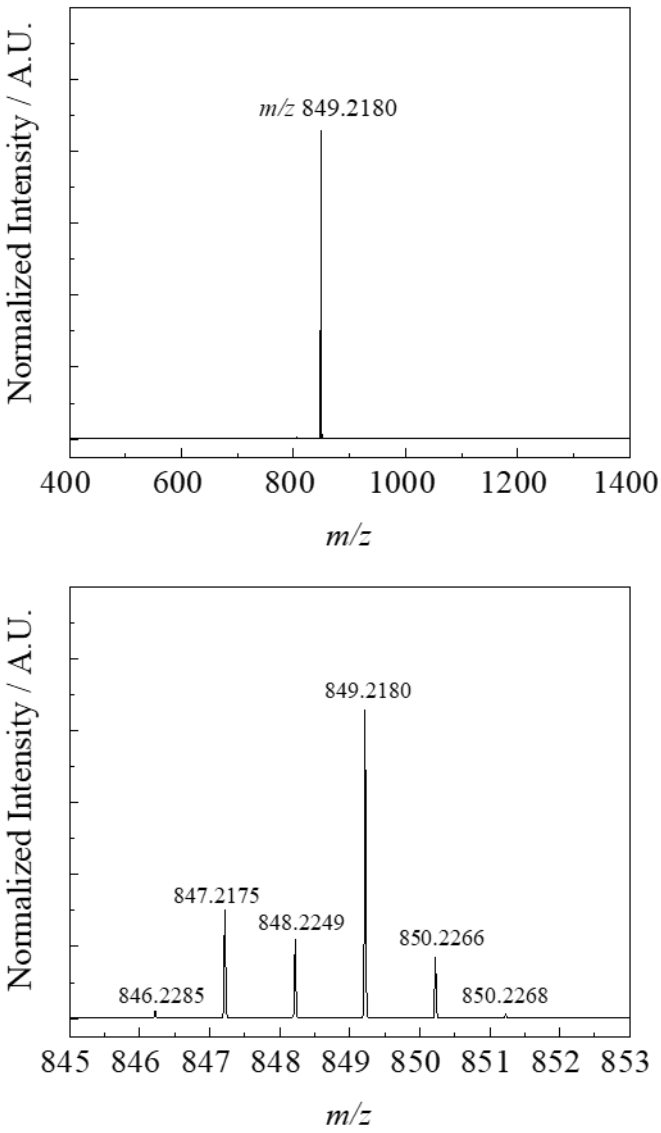

Fig. S22 ^{1}H NMR spectrum of complex **1b** in DMSO-d_6 at 298 K.

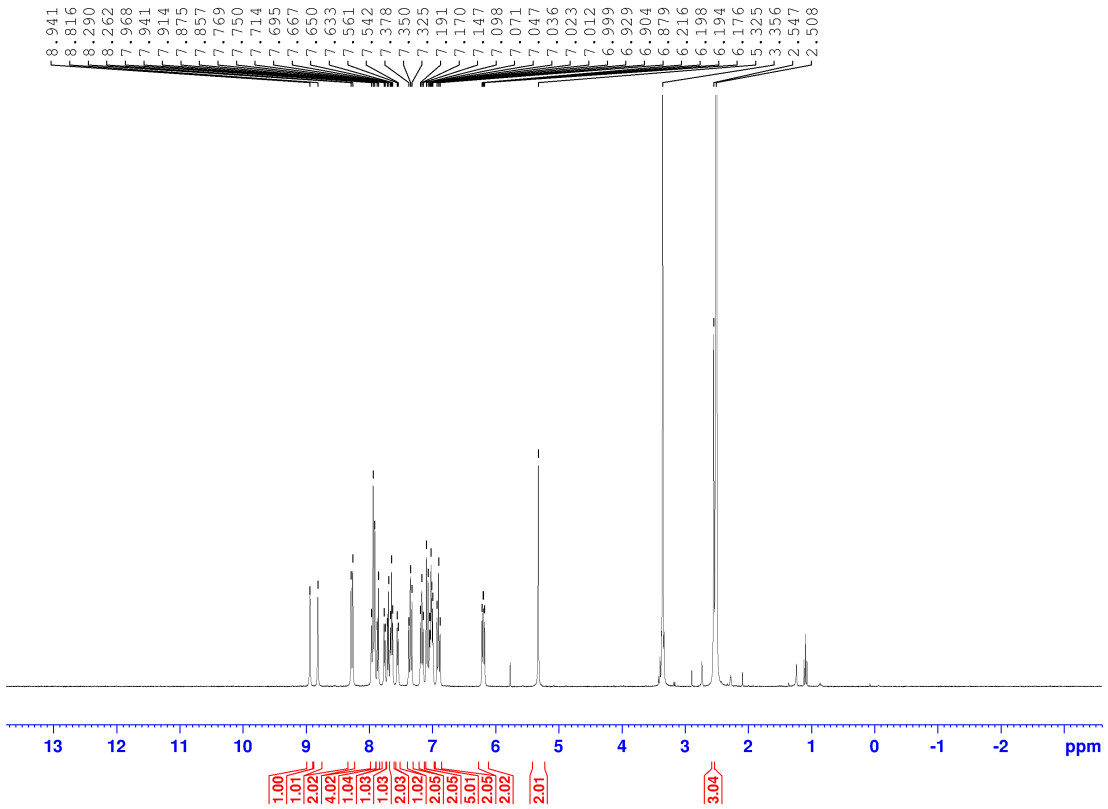

Fig. S23 ^{13}C NMR spectrum of complex **1b** in DMSO-d_6 at 298 K.

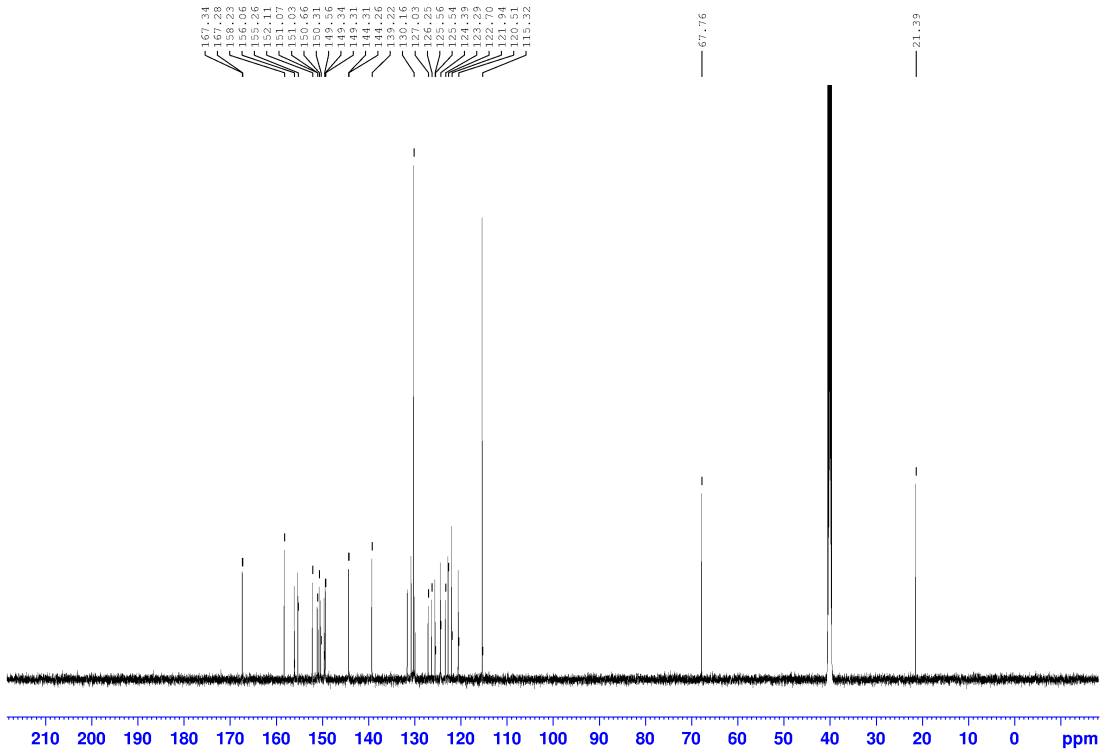

Fig. S24 HR-ESI-mass spectra of complex **1b** in CH_3CN.

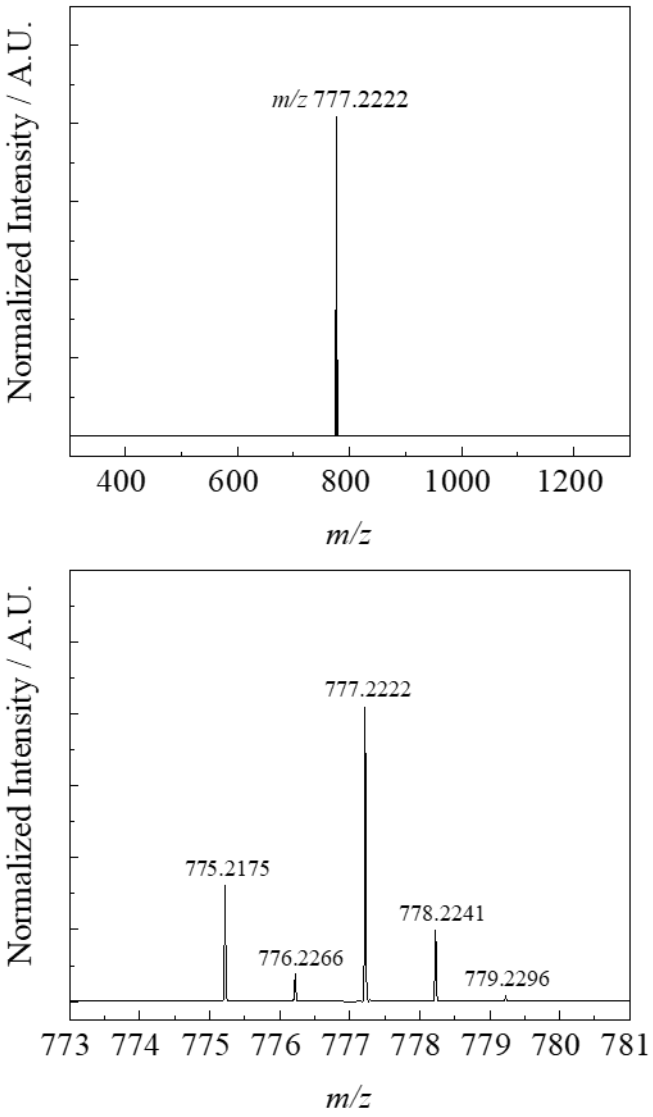

Fig. S25 ^{1}H NMR spectrum of complex **2a** in DMSO-d_6 at 298 K.

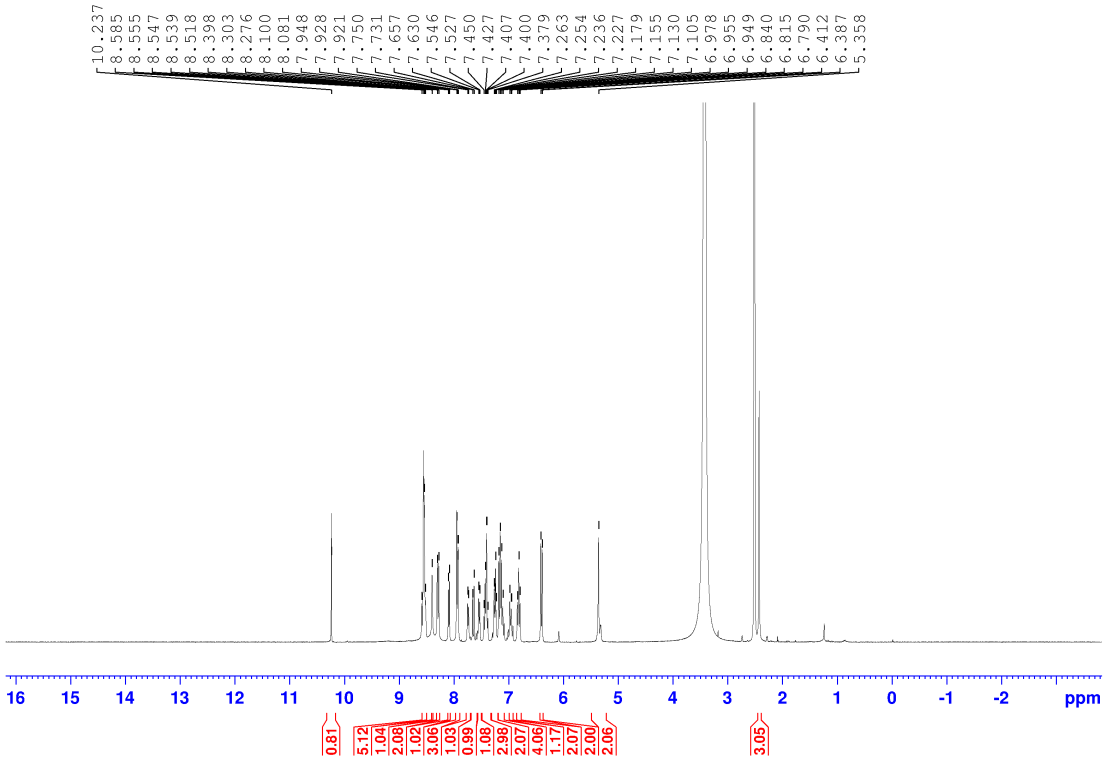

Fig. S26 ^{13}C NMR spectrum of complex **2a** in DMSO-d_6 at 298 K.

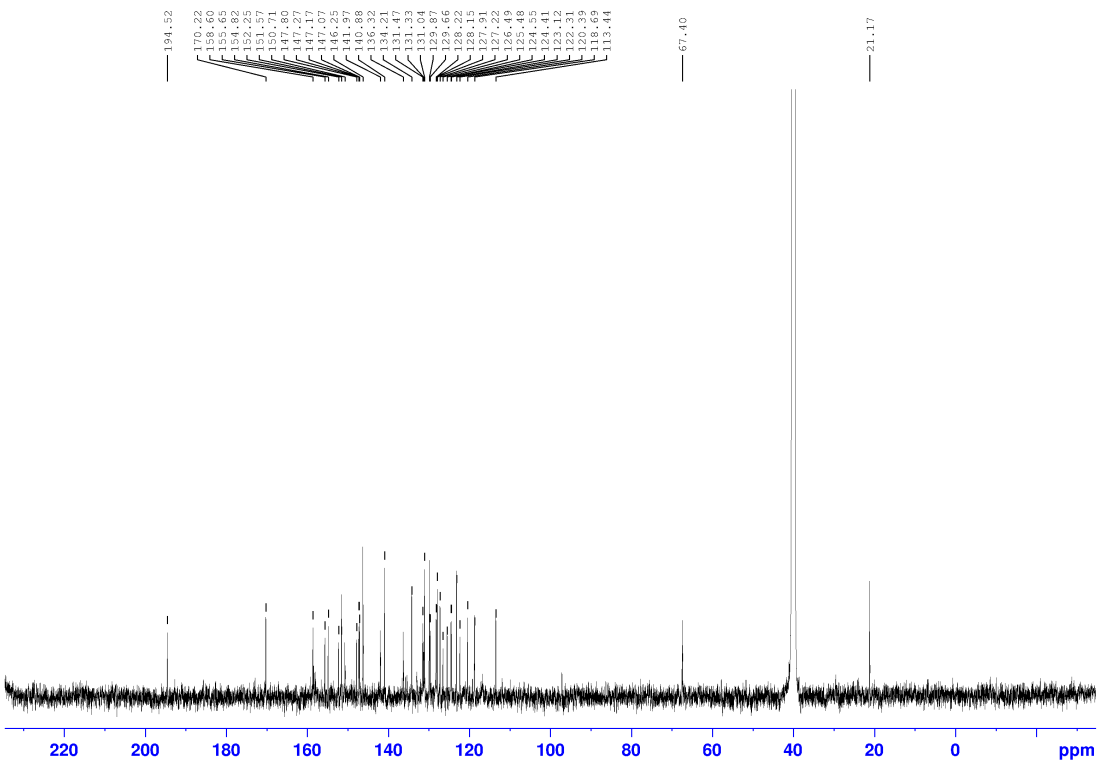

Fig. S27 HR-ESI-mass spectra of complex **2a** in CH_3CN.

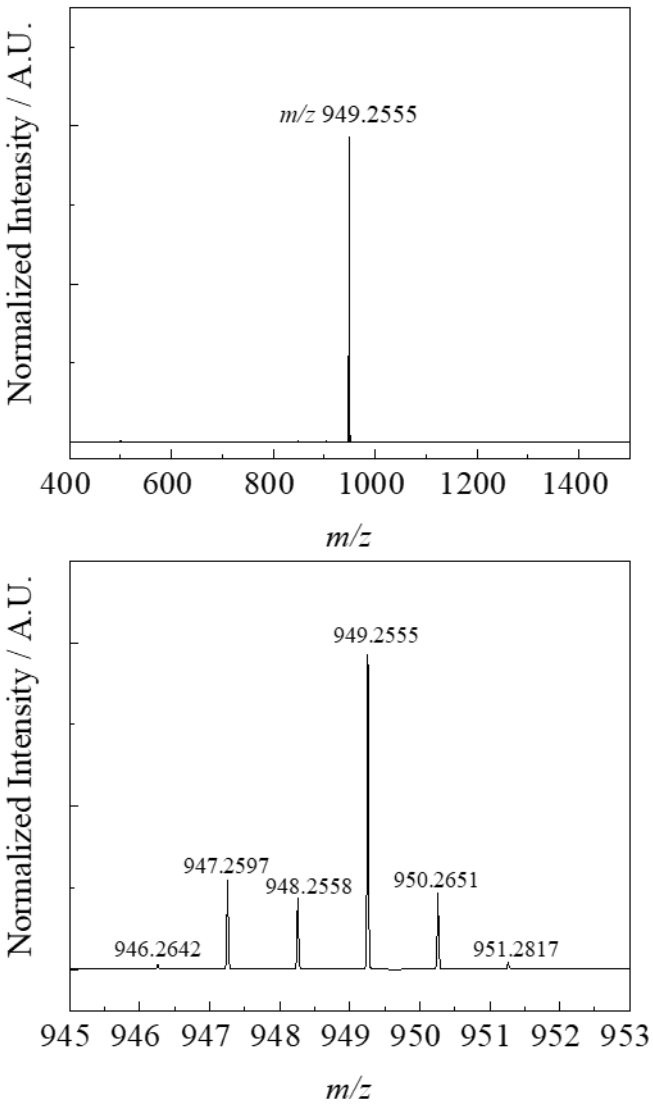

Fig. S28 ^{1}H NMR spectrum of complex **2b** in acetone-d_6 at 298 K.

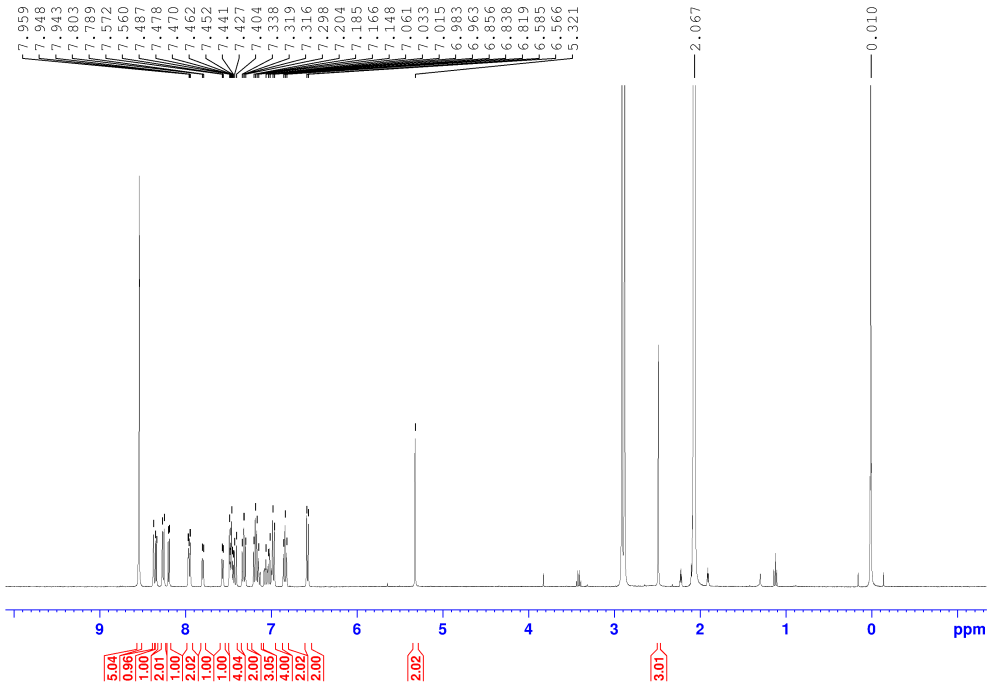

Fig. S29 ^{13}C NMR spectrum of complex **2b** in DMSO-d_6 at 298 K.

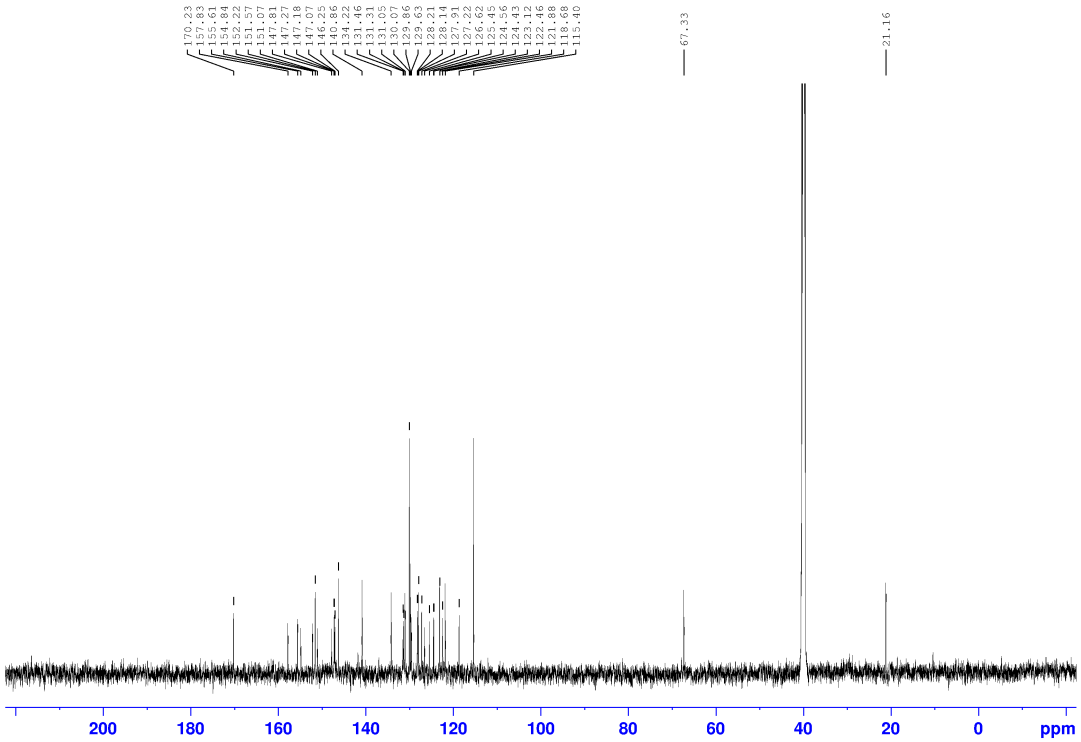

Fig. S30 HR-ESI-mass spectra of complex **2b** in CH_3CN.

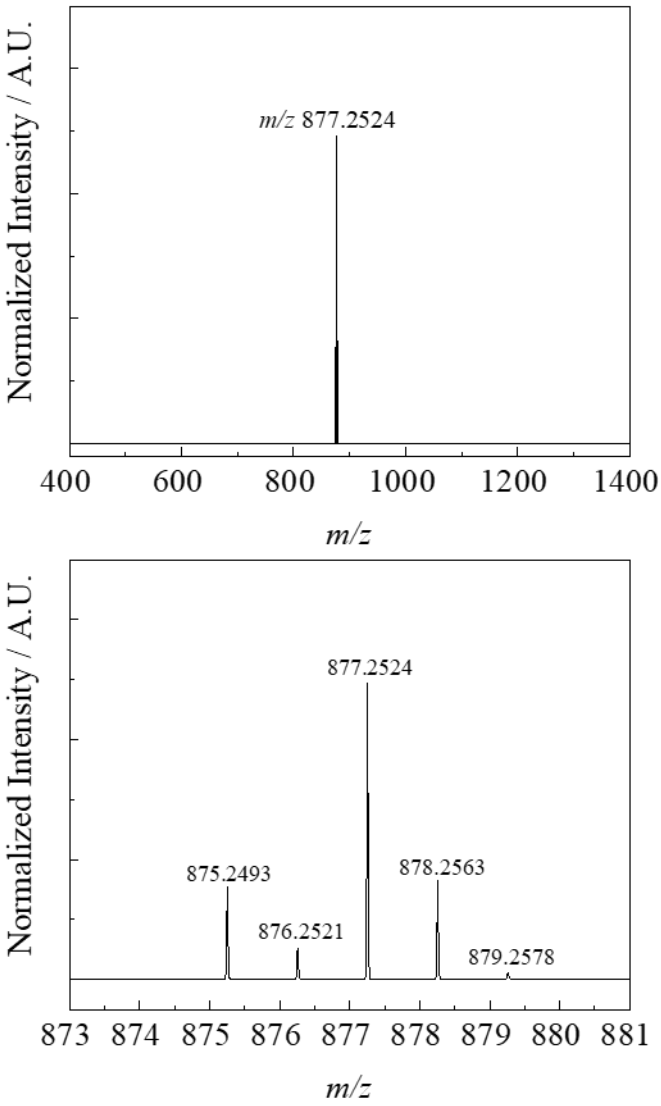

Fig. S31 ^{1}H NMR spectrum of complex **3a** in DMSO-d_6 at 298 K.

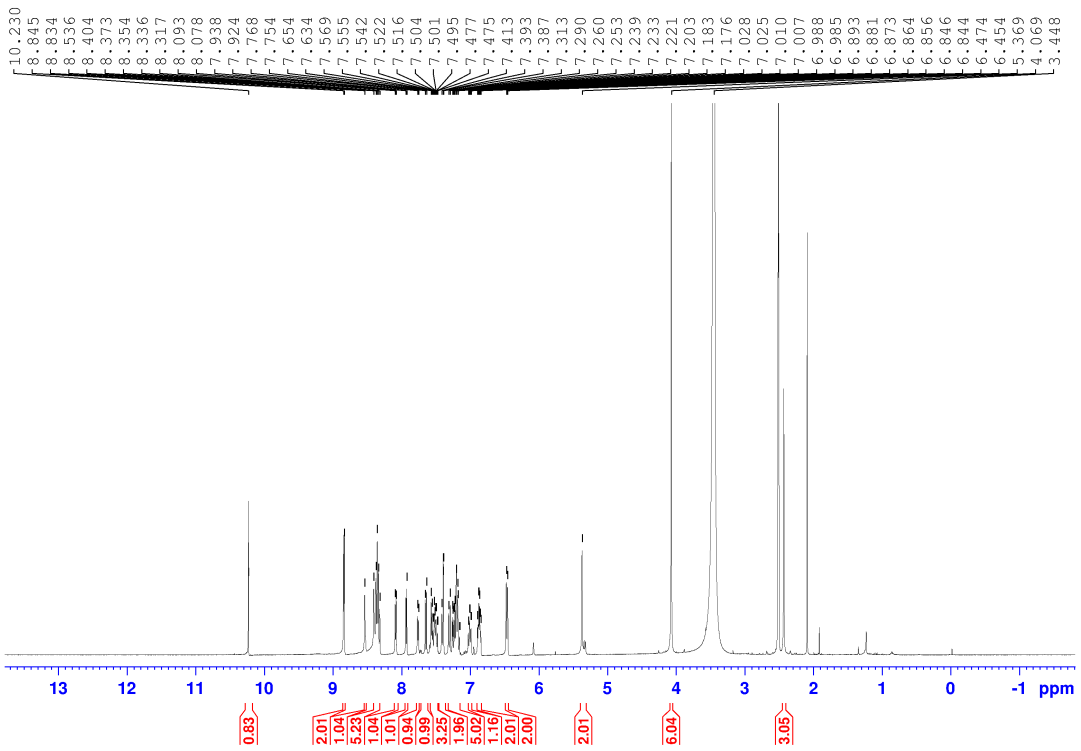

Fig. S32 ^{13}C NMR spectrum of complex **3a** in DMSO-d_6 at 298 K.

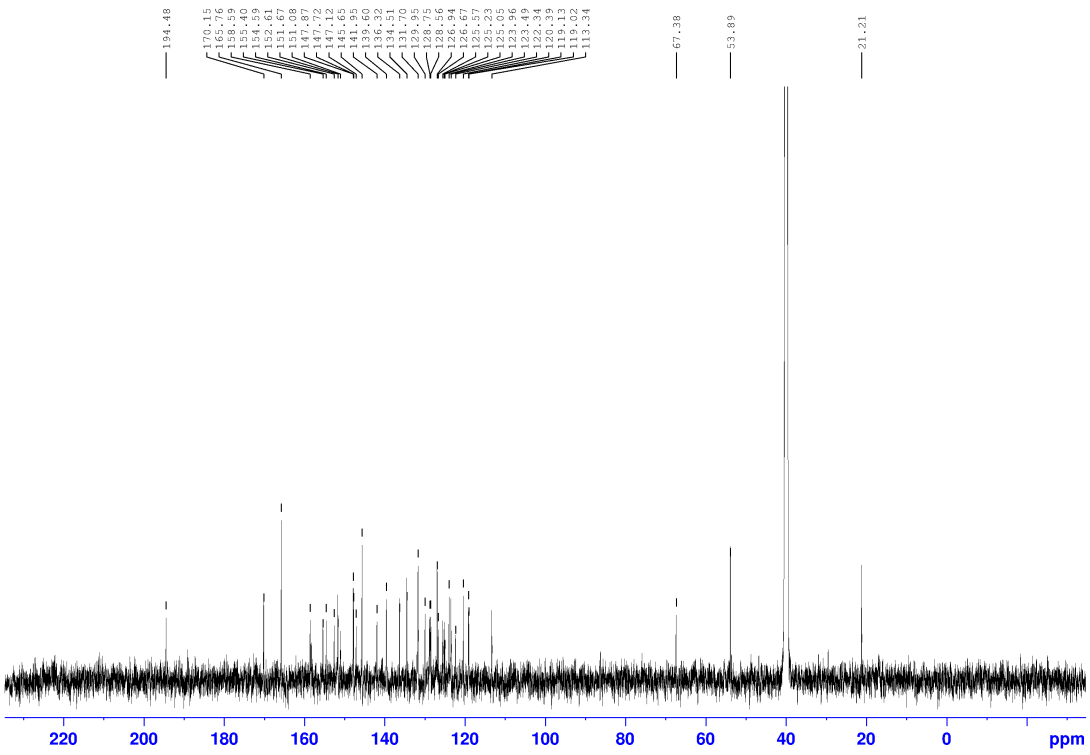

Fig. S33 HR-ESI-mass spectra of complex **3a** in CH_3CN.

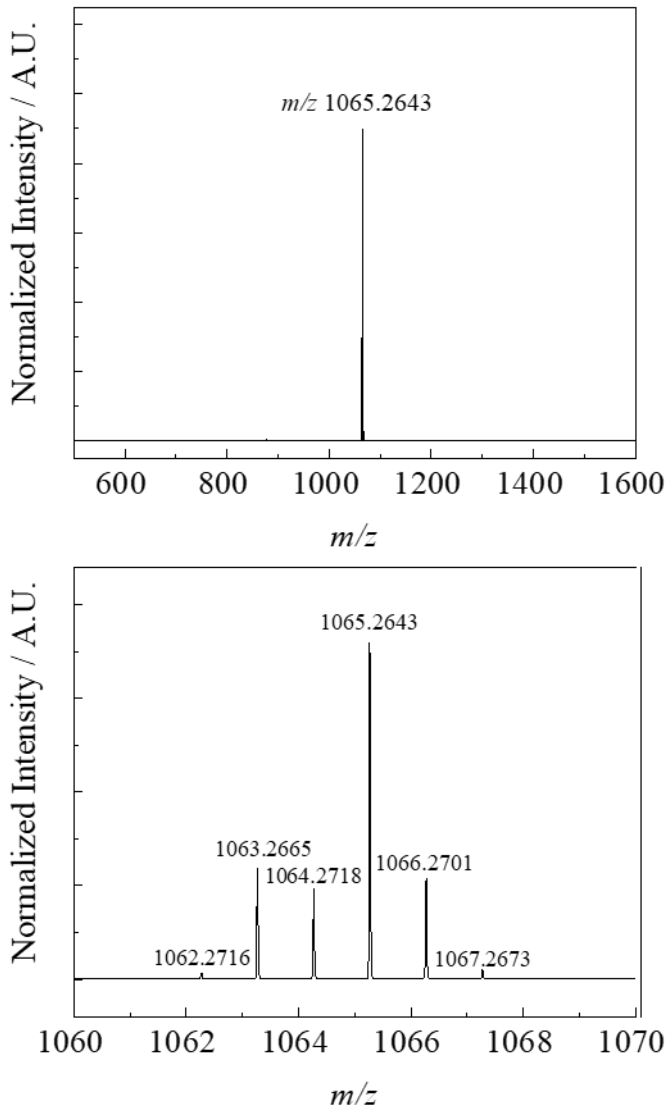

Fig. S34 ^{1}H NMR spectrum of complex **3b** in acetone-d_6 at 298 K.

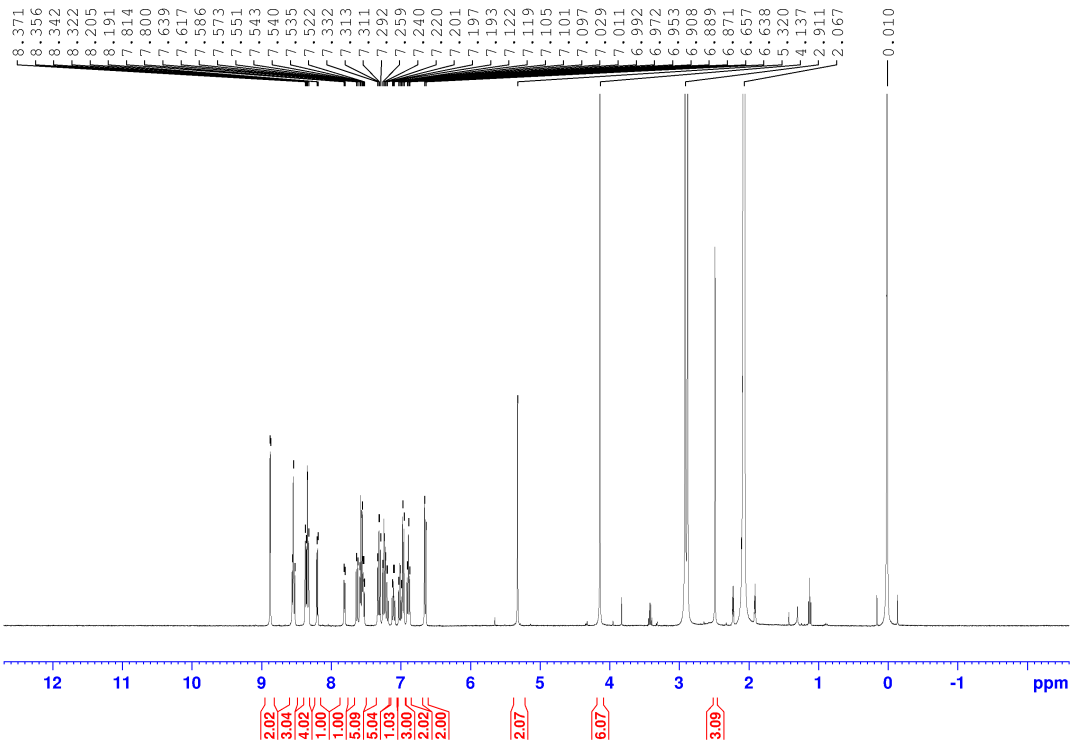

Fig. S35 ^{13}C NMR spectrum of complex **3b** in DMSO-d_6 at 298 K.

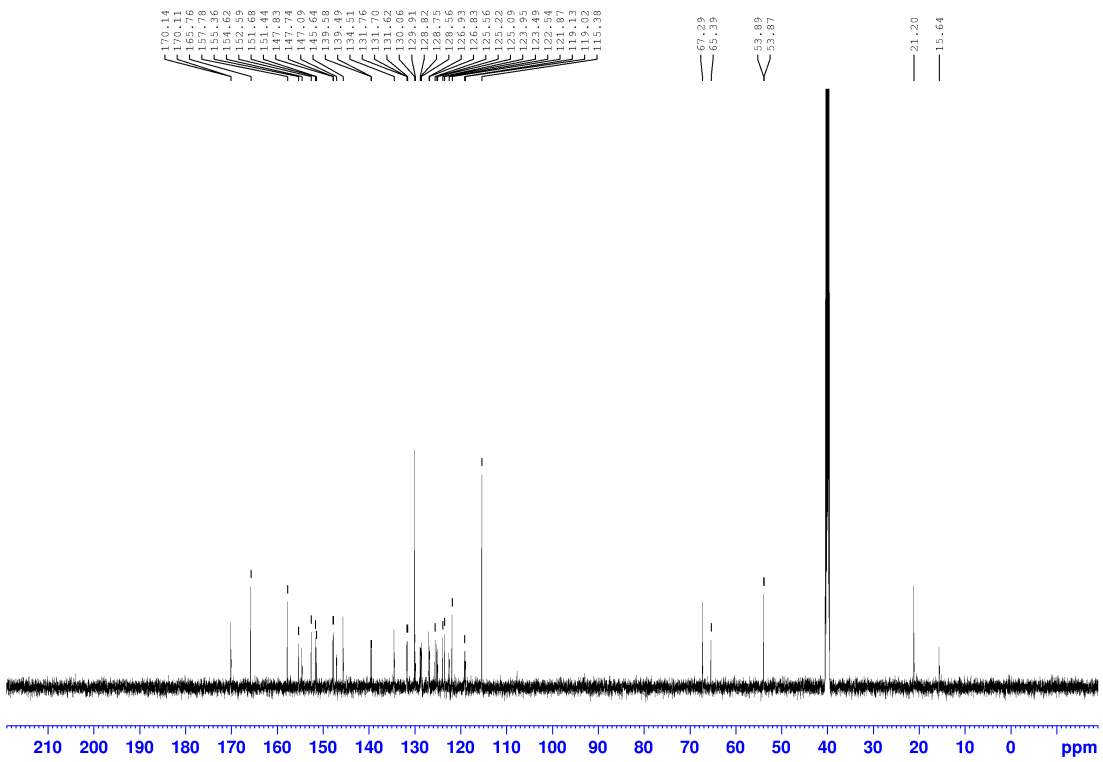

Fig. S36 HR-ESI-mass spectra of complex **3b** in CH_3CN.

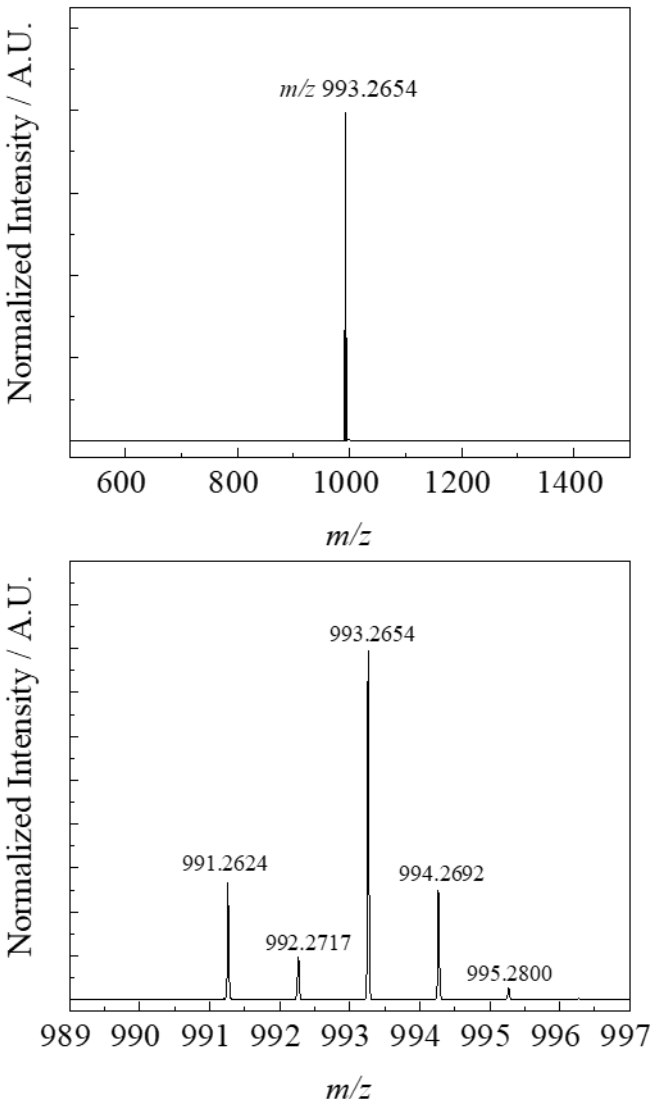

References

1. W. L. F. Armarego, C. Chai, *Purification of Laboratory Chemical*, 7th ed, Butterworth-Heinemann, Oxford, 2013, pp. 103 – 554.
2. T. S.-M. Tang, K.-K. Leung, M.-W. Louie, H.-W. Liu, S. H. Cheng and K. K.-W. Lo, *Dalton Trans.*, 2015, **44**, 4945.
3. B. D. Sherman, Y. Xie, M. V. Sheridan, D. Wang, D. W. Shaffer, T. J. Meyer and J. J. Concepcion, *ACS Energy Lett*., 2017, **2**, 124.
4. L. Huang, P. K.-K. Leung, L.C.-C. Lee, G.-X. Xu, Y.-W. Lam and K. K.-W. Lo, *Chem. Commun.,* 2022, **58**, 10162.
5. E. Sella and D. Shabat, *Org. Biomol. Chem*., 2013, **11**, 5074.
6. S. Sprouse, K. A. King, P. J. Spellane and R. J. Watts, *J. Am. Chem. Soc*., 1984, **106**, 6647.
7. K. Suzuki, A Kobayashi, S. Kaneko, K. Takehira, T. Yoshihara, H. Ishida, Y. Shiina, S. Oishi and S. Tobita, *Phys. Chem. Chem. Phys.,* 2009, **11**, 9850.
8. M. Martínez-Alonso, N. Busto, L. D. Aguirre, L. Berlanga, M. C. Carrión, J. V. Cuevas, A. M. Rodríguez, A. Carbayo, B. R. Manzano, E. Ortí, F. A. Jalón, B. García and G. Espino, *Chem. Eur. J.,* 2018, **24**, 17523.
9. D. Garcìa-Fresnadillo, Y. Georgiadou, G. Orellana, A. M. Braun and E. Oliveros, *Helv. Chim. Acta*, 1996, **79**, 1222.
10. M. J. Forkink, A. M. Smeitink, R. Brock, P. H. G. M. Willems and W. J. H. Koopman, *Biochim. Biophys. Acta,* 2010, **1797**, 1034.
11. X. Gong, Y. Didan, J. G. Lock and S. Strömblad, *EMBO J*., 2018, **37**, e98994.
12. L. C. Crowley, B. J. Marfell and N. J. Waterhouse, *Cold Spring Harbor Protoc.,* 2016, **2016**, 778.

13. N. E. Saris, V. V. Teplova, I. V. Odinokova and T. S. Azarashvily, *Anal. Biochem.,* 2004, **328**, 109.